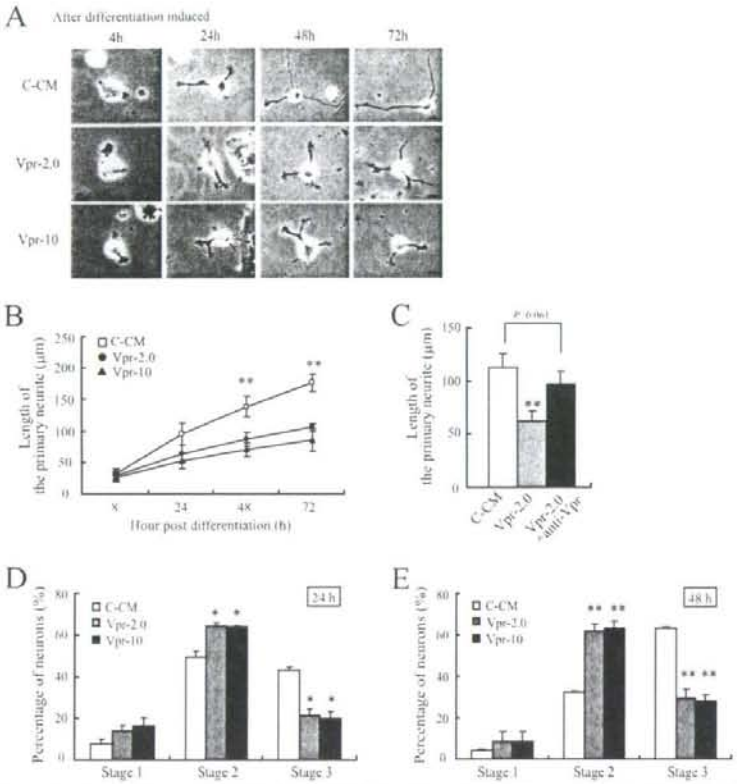

FIG. 2. Axonal malformation by Vpr in neuronal cells. (A) C-CM, Vpr-2.0, and Vpr-10 were used in differentiation cultures of neuronal progenitor cells, and neurite outgrowth was monitored for 72 h. Phase-contrast images were obtained using a 40× objective. Scale bars, 20 μm. (B) The lengths of the primary neurites of the neurons were measured. **, $P < 0.01$ compared to results for C-CM culture. (C) The length of the primary neurites of neurons cultured with C-CM, Vpr-2.0, or rVpr together with anti-Vpr antibody (Vpr-2.0+anti-Vpr) were measured. **, $P < 0.01$ compared to results for culture with C-CM or Vpr-2.0+anti-Vpr. (D and E) Progenitor cells under each condition were classified into three developmental stages at 24 h (D) and 48 h (E) in culture as described above. **, $P < 0.01$ compared to results for C-CM culture.

depletion of ATP concentration were induced by rVpr treatment, there was no significant difference in the percentages of progenitor cells expressing activated caspase-3 between 2.0 pM rVpr-treated cells and C-CM-treated cells (Table 1). Although apoptosis was not detected in progenitor cells cultured with low concentrations of rVpr (0.2, 2.0, and 10 pM), at higher concentrations of rVpr (100 pM or 1.0 nM), the differentiation of progenitor cells was arrested at stage 1 or early in stage 2 (data not shown), and many cells expressed activated caspase-3 (Table 1).

It has been shown that the depolarization of the mitochondrial membrane potential and the inhibition of ATP synthesis cause mitochondrial transport to slow down (10, 46). To measure the velocity of mitochondrial movement within neurites or axons, progenitor cells left untreated or treated with rVpr were stained for mitochondria using MitoTracker. We detected severely suppressed mitochondrial transport within neurites in 2.0 pM rVpr-treated cells (Fig. 3C, column b) compared to that of neurites cultured in C-CM (Fig. 3C, column a). As shown in Fig. 3D, the calculated velocity of mitochondrial transport in 2.0 pM rVpr-treated cells was slower than that in C-CM-treated cells (0.10 ± 0.02 μm/s and 0.31 ± 0.04 μm/s, respectively). These results suggest that Vpr induces abnormality in mitochondria transportation through the suppression of ATP synthesis.

To elucidate the effect of mitochondrial transport inhibition in mitochondrial localization, cells treated with serially increasing concentrations of rVpr were stained with antibody against cytochrome *c*, a mitochondrial inner membrane protein. As shown in Fig. 3E, the localization of mitochondria in primary neurites of cells seemed to be altered and reduced when the progenitor cells were treated with rVpr at concentrations above 0.2 pM. Although rVpr did not affect the total mitochondrial content in each live cell as shown by MitoTracker staining (Fig. 3F), the mitochondrial content in neurites of rVpr-treated cells was significantly reduced (Fig. 3G), indicating that the amount of mitochondrial content decreased predominantly within neurites in the presence of rVpr, and this might be caused by the retardation of mitochondrial transportation.

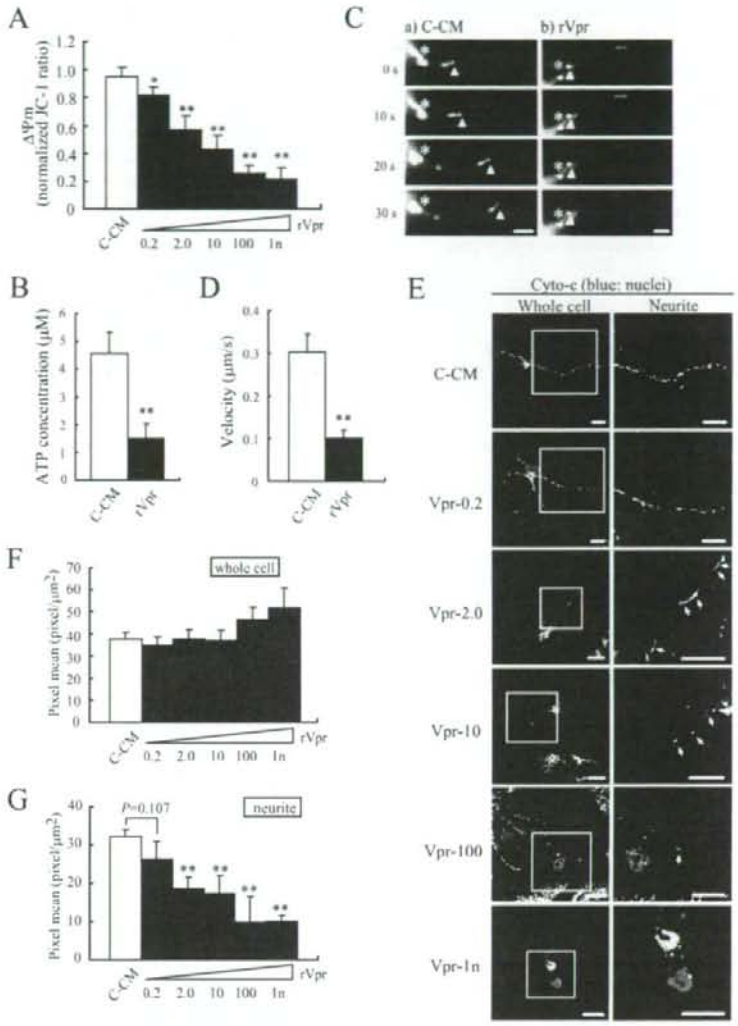

FIG. 3. Mitochondrial dysfunction caused by treatment with Vpr. (A) C-CM, Vpr-0.2, Vpr-2.0, Vpr-10, Vpr-100, and Vpr-1n were added to differentiation cultures of neuronal progenitor cells. Cells cultured in each medium were stained with JC-1, and the $\Delta\Psi m$ was calculated as described in Materials and Methods. *, $P < 0.05$ compared to the results for C-CM culture; **, $P < 0.01$ compared to the results for C-CM culture. (B) The cellular ATP concentration of progenitor cells cultured in C-CM or 2.0 pM rVpr (rVpr) was measured. **, $P < 0.01$ compared to the results of C-CM culture. (C) Neuronal progenitor cells cultured in C-CM (column a) or 2.0 pM rVpr (column b) were stained with MitoTracker. Images were acquired every 10 s using a 63× objective. Asterisks indicate stationary mitochondria, and arrowheads indicate moving mitochondria within neurites. Scale bars, 5 μm. (D) The velocity of mitochondrial transportation within neurites under each condition was calculated as described in Materials and Methods. **, $P < 0.01$ compared to the results for C-CM culture. (E) Mitochondria in progenitor cells cultured in each condition were stained using antibody against cytochrome *c* (Cyto-c; green), and nuclei were stained by Hoechst 33342 (blue), as described in Materials and Methods. Rectangular regions were enlarged and are shown in the right panels. Arrows indicate mitochondrial compartments within neurites. Confocal images were obtained using a 63× objective. Scale bars, 20 μm. (F and G) Progenitor cells treated with or without a serial dilution of rVpr as described above were stained with MitoTracker, and the mean pixels of whole cells (F) or neurites (G) were quantified. **, $P < 0.01$ compared to the results for C-CM culture.

Correlation between rVpr-induced mitochondrial membrane depolarization and developmental retardation of neuronal progenitor cells. We used Vpr recombinant mutants that have a strong, a moderate, or no ability to caused mitochondrial membrane depolarization to study the correlation between Vpr-mediated $\Delta\Psi m$ reduction and developmental arrest. As shown in Fig. 4A, one C-terminal deletion mutant of rVpr protein containing amino acids (aa) 1 to 84 (rVpr-ΔC12),

TABLE 1. Vpr-induced apoptosis in neuronal cells

Condition	Concn of Vpr (pM)	% of neuronal cells expressing activated caspase-3
C-CM	0	5.83 ± 0.97
Vpr-0.2	0.2	6.23 ± 2.04[a]
Vpr-2.0	2	7.12 ± 3.08[a]
Vpr-10	10	8.60 ± 1.80[a]
Vpr-100	100	14.69 ± 2.71[b]
Vpr-1n	1,000	17.33 ± 0.42[b]

[a] There was no significant difference between results for the indicated condition and those for C-CM.
[b] $P < 0.01$ compared to results for C-CM.

which is defective in DNA binding (54), was used, and three point mutants of rVpr were used, including R80A, which moderately induces mitochondrial membrane depolarization (25); I81A, which was used as a negative control; and R73, 77, 80A, which cannot induce mitochondrial membrane depolarization (25). We treated the progenitor cells with each mutant rVpr at 2.0 pM and measured the $\Delta\Psi$m in the treated cells. Although the suppression of $\Delta\Psi$m by rVpr-ΔC12 or rVpr-I81A was similar to that by rVpr-WT, the suppression by rVpr-R80A was clearly less than that by rVpr-WT (Fig. 4B). Furthermore, as shown in Fig. 4B, a triple-amino-acid mutant (rVpr-R73, 77, 80A) did not have any ability to cause mitochondrial membrane depolarization. These results confirmed that R73, R77, and R80 are critical amino acids for the induction of mitochondrial membrane depolarization, as described previously (25).

To determine the correlation between the mitochondrial membrane potential and neuronal development, neuronal progenitor cells treated with those mutants at a constant concentration (2.0 pM) were classified into three developmental stages at 48 h in culture as described in Materials and Methods. As shown in Fig. 4C, the classification profiles of rVpr-ΔC12- and rVpr-I81A-treated cells were almost identical to that of rVpr-WT-treated cells. However, in rVpr-R80A-treated cells, less developmental retardation was found and a significantly higher percentage of cells were in stage 3 compared to that for rVpr-WT-treated cells. Furthermore, in rVpr-R73, 77, 80A-treated cells, no developmental arrest was found, as shown by the very similar classification profile compared to that of the control profile. These results show that there may be a positive correlation between the ability of a Vpr mutant to cause membrane depolarization and its ability to cause developmental arrest.

As shown in Fig. 4D, a small but convincing amount of Vpr was detected in the ANT-containing mitochondrion fraction but not in the cytosolic fraction in neuronal progenitor cells treated with 2.0 pM rVpr-WT. This suggests that Vpr has the tendency to accumulate in mitochondria of neuronal progenitor cells. Similar amounts of rVpr-R73, 77, 80A and rVpr-WT were found to be in the mitochondria of the treated cells. However, no cytoplasmic cytochrome *c* was found in cells treated with a high concentration of rVpr-R73, 77, 80A. In addition, a large amount of cytochrome *c* release was found in cytosolic fractions in cells treated with a high concentration (1.0 nM) of rVpr-WT, but the release of cytochrome *c* was hardly found in cells treated with 2.0 pM of rVpr.

To confirm that the observed effects were indeed caused by rVpr, several Vpr deletion mutant peptides were used at a constant concentration (2.0 pM). The Vpr deletion mutant peptides we used were C45 (aa 53 to 96) (38), C45D18 (aa 53 to 78) (38, 55), LR20 (aa 62 to 81), and LR17 (aa 62 to 78) (Fig. 4A). As shown in Fig. 4B, the $\Delta\Psi$m suppression by C45 and LR20 was similar to that by rVpr-WT, but the suppression by C45D18 and LR17 was clearly weaker. In addition, as shown in Fig. 4C, the developmental classification profiles of C45- and LR20-treated cells were almost identical to that of rVpr-WT-treated cells. However, C45D18- and LR17-treated cells had significantly decreased abilities to induce developmental retardation. These results suggest that Vpr deletion mutant peptides have the same abilities to cause mitochondrial membrane depolarization and developmental retardation that rVpr mutants have. The abilities of the Vpr deletion mutant peptides to cause developmental arrest also were dependent on their ability to cause mitochondrial membrane depolarization.

Protection against rVpr-induced mitochondrial dysfunction by UQ. We found that mitochondrial membrane depolarization might induce the inhibition of neuronal development. To reveal the direct effect of mitochondrial membrane depolarization on neuronal development, neuronal cells were treated with an inhibitor of membrane depolarization along with rVpr-WT. UQ, which is a ubiquinone analogue that protects mitochondrial membranes against depolarization by closing the mitochondrial permeability transition pore (mPTP), was used. First, to confirm the specificity of UQ for the inhibition of membrane depolarization, neuronal cells were treated with FCCP, which induces mitochondrial membrane depolarization and inhibits mitochondrial movement within axons (46), in the presence or absence of UQ. At 48 h of culture, the morphology of cells treated with FCCP was very similar to that of cells treated with 2.0 pM rVpr (data not shown). As shown in Fig. 5A, mitochondrial membrane depolarization was induced in neuronal progenitor cells treated with FCCP (100 μM). In progenitor cells simultaneously treated with FCCP and UQ (100 μM), the mitochondrial membrane potential was clearly sustained. Next, we added UQ to cultures of neuronal progenitor cells treated with rVpr (2.0 pM). UQ protected the progenitor cells against depolarization and significantly restored the membrane potential (Fig. 5A). Although membrane depolarization was suppressed with treatment using UQ, no significant recovery was found in cells treated with the caspase-3 inhibitor z-DEVD-fmk (100 μM) or with ATP (10 μM). Similarly, ATP production was not rescued by treatment using z-DEVD-fmk (2.53 ± 0.43 μM) (Fig. 5B). In contrast, when UQ was used, the ATP concentration (3.06 ± 0.36 μM) was restored to the proximity of the control value (3.64 ± 0.30 μM) (Fig. 5B). Treatment with both UQ and z-DEVD-fmk seemed to increase ATP synthesis, although this increase was not found to be statistically significant compared to ATP synthesis with UQ treatment alone.

We next measured the velocity of the transportation of mitochondria in neurites or axons using MitoTracker. We showed severely suppressed mitochondrial transport within the neurites in rVpr-treated cells (Fig. 3C and D). As shown in Fig. 5C, although the addition of z-DEVD-fmk to rVpr-treated cells could not restore the velocity of mitochondrial transport (0.12 ± 0.02 μm/s), the addition of UQ or both UQ and z-DEVD-fmk to rVpr-treated cells restored the velocity of mitochondrial transport (0.17 ± 0.01 and 0.19 ± 0.02 μm/s, respectively), indicating that the transportation of mitochon-

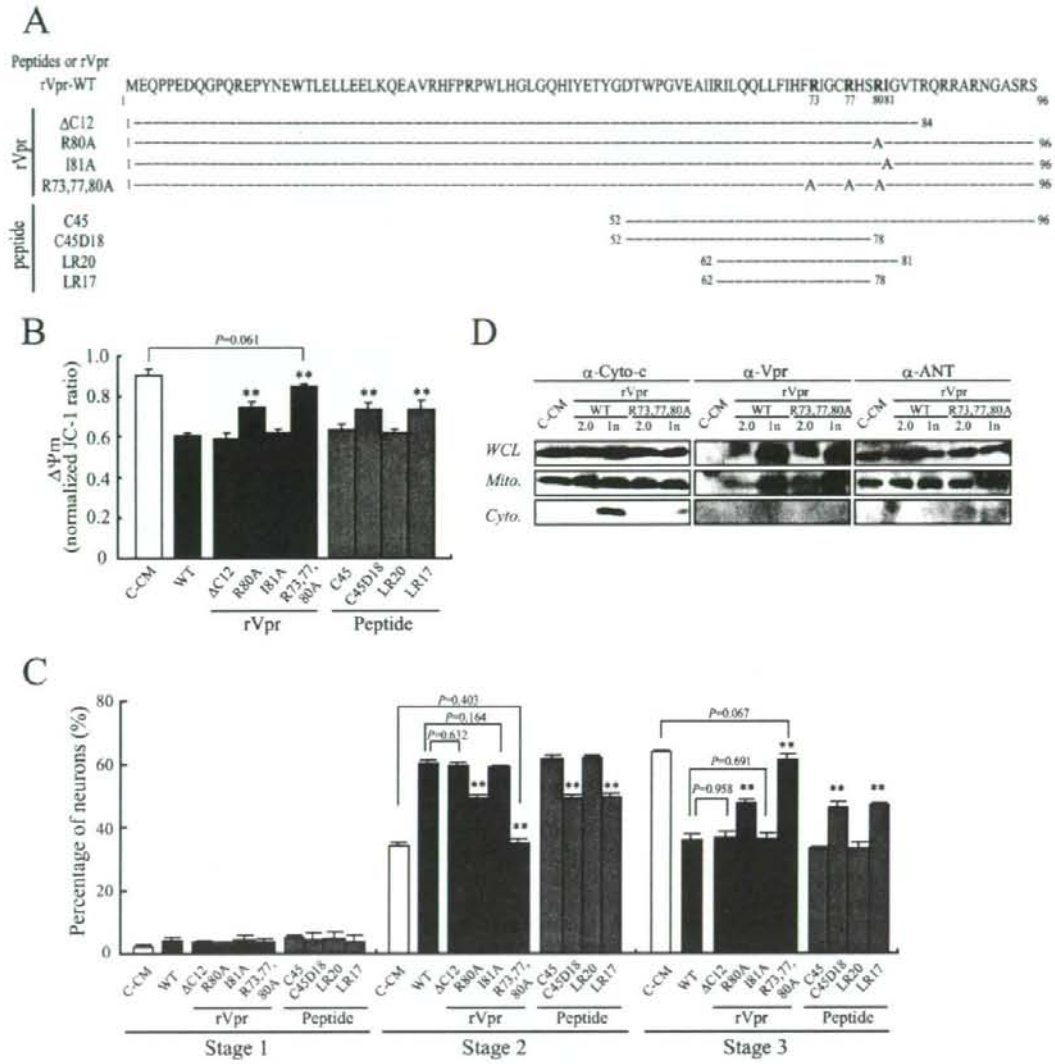

FIG. 4. Inhibition of neuronal development caused by rVpr-induced mitochondrial membrane depolarization. (A) The amino acid sequences of Vpr mutants are displayed. The amino acid sequence of rVpr-WT is depicted at the top. The Vpr deletion mutant peptides and recombinant mutant proteins are listed below, with horizontal lines depicting unaltered sequences and numbers delineating the first or last amino acid of each mutant. The alanines that replace each residue are indicated. (B) Progenitor cells treated with C-CM or with 2.0 pM rVpr-WT (WT), four rVpr mutants (ΔC12; R80A; I81A; and R73, 77, 80A) or four Vpr mutant peptides (C45, C45D18, LR20 and LR17) were stained with JC-1, and the $\Delta\Psi$m values were calculated as described in the text. **, $P < 0.01$ compared to results for rVpr-WT. (C) Cells cultured in each condition (2.0 pM) were classified into three developmental stages as described above. **, $P < 0.01$ compared to results for rVpr-WT. (D) Cells were cultured in C-CM or rVpr-WT (2.0 pM and 1.0 nM; rVpr-WT-2.0 and rVpr-WT-1n, respectively) or rVpr-R73, 77, 80A (2.0 pM and 1.0 nM; rVpr-R73, 77, 80A-2.0 and rVpr-R73, 77, 80A-1n, respectively). The mitochondrial fraction (*Mito.*) and cytosolic fraction (*Cyto.*) were separated, and anti-cytochrome *c* (α-Cyto-c), anti-Vpr (α-Vpr), or anti-ANT (α-ANT) antibody in individual fractions or whole-cell lysates (*WCL*) was detected by Western blotting using each antibody.

dria within neurites was restored by the treatment of UQ through the restoration of ATP production, followed by the inhibition of mitochondrial membrane depolarization.

To examine the protective capability of UQ against Vpr-induced developmental retardation, neuronal progenitor cells were classified into three developmental stages. When only caspase-3 inhibitor (z-DEVD-fmk) was added to CM of 2.0 pM Vpr-treated cells, the majority of neuronal cells were retained

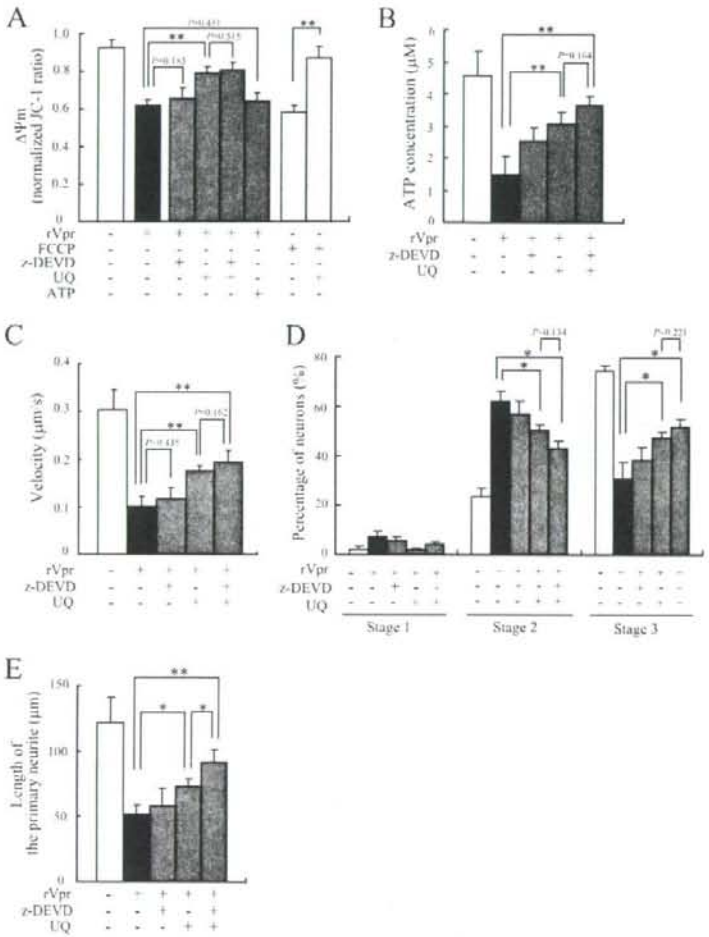

FIG. 5. Restoration of mitochondrial dysfunction by treatment with UQ. (A) The $\Delta\Psi m$ of progenitor cells cultured in C-CM or in the presence of 2.0 pM rVpr or 100 μM FCCP was calculated as described in Materials and Methods. **, $P < 0.01$. (B) The cellular ATP concentration of cells cultured in C-CM or in the presence of 2.0 pM rVpr (rVpr) was measured. **, $P < 0.01$. (C) The velocity of mitochondrial transportation within neurites or axons under each condition was calculated. **, $P < 0.01$. (D) Cells cultured under each condition were classified into three developmental stages as described in the text. *, $P < 0.05$. (E) The lengths of the primary neurites of cells cultured under each condition were measured. *, $P < 0.05$; **, $P < 0.01$. In all experiments, 100 μM z-DEVD-fmk (z-DEVD), 100 μM UQ, and 10 μM ATP were used.

at stage 2, as was the case for cells treated with Vpr alone. However, after treatment with UQ or both UQ and z-DEVD-fmk, a significant fraction of Vpr-treated cells proceeded to stage 3 (Fig. 5D), suggesting that the recovery of mitochondrial transportation induced by UQ treatment allowed for the development of neurons. Furthermore, to determine the ability of UQ to restore neurite outgrowth, the length of the primary neurite of neuronal cells was measured at 48 h after the initiation of differentiation. When UQ was added to 2.0 pM Vpr-treated cells, the mean length of primary neurites was significantly longer than that of cells treated with Vpr alone or also with z-DEVD-fmk (Fig. 5E). Interestingly, the rescue of axonal growth was more efficient when UQ and z-DEVD-fmk were added together than when only UQ was added ($P < 0.05$).

Protective effect of UQ on neuronal development in organotypic hippocampal slice cultures. To better simulate the effect of soluble Vpr on neuronal precursor cells in vivo and to characterize the ability of the caspase-3 inhibitor and UQ to rescue neuronal development from Vpr-induced abnormalities, we employed rat organotypic hippocampal slice cultures. In organotypic hippocampal slice cultures, neurons are maintained in microenvironments that are very similar to those found in vivo (17). Not only the extracellular architect but also the synaptodendritic interactions are reconstituted in slice cul-

tures (18). In addition, the presence of neurogenesis has been reported to happen in hippocampal slice cultures (28, 45). For these reasons, slice cultures have been used widely to study the morphology and plasticity of the hippocampus. The typical cellular arrangement of granule cells was reconstituted in slices on porous membranes 14 days after the initiation of culture. Slices then were cocultured with HIV-1_{JRFL}-infected MDM or uninfected MDM across the porous membrane or were exposed to rVpr (2.0 pM). From the examination of B3T, a neuronal cell marker, and NFP expression using immunofluorescence, we found that the number of axons severely decreased in the slices exposed to HIV-1-infected MDM or rVpr (Fig. 6A and B). In addition, in the slices exposed to HIV-1-infected MDM or rVpr, the expression of MAP2, a marker for the neuronal dendritic network, was severely disturbed (Fig. 6A and B). We also found atrophy and the beading of dendrites (Fig. 6A), indicating that postsynaptic structures also were severely disrupted. These results suggest that HIV-1-infected MDM or Vpr induce axonal and dendritic malformation in organotypic hippocampal slice cultures.

Intrinsic and spontaneous neurogenesis are reported to take place at the DG in organotypic hippocampal slice cultures (28, 45). To investigate the dysfunction of neuronal cell development in hippocampal slice cultures exposed to HIV-MDM or rVpr, we labeled endogenous precursor cells in the slices using an EGFP-expressing MLV vector (SRα-EGFP). The virus vector was microinjected into the suprapyramidal region of the GCL as described before (28). Since MLV only infects dividing cells and its DNA is incorporated into the host DNA, only newly divided cells express EGFP. After inoculation with SRα-EGFP, slices were exposed to HIV-1-infected MDM, uninfected MDM, or rVpr in the presence or absence of caspase-3 inhibitor (z-DEVD-fmk), UQ, or both. During daily observations of the inoculated areas under a fluorescent microscope, we found many EGFP-expressing cells (data not shown). The numbers of the EGFP-expressing cells increased for 2 weeks postinoculation in all slices (data not shown). To observe the morphology, the slices were fixed and examined by confocal microscopy. EGFP-expressing cells typically were detected in and around the GCL area. Most cells possessed one elongated axon and several dendrite-like processes in slices cultured with or without uninfected MDM (Fig. 7A, rows a and b). In contrast, in slices exposed to HIV-1-infected MDM or rVpr alone, most $EGFP^+$ cells possessed minor neurites with similar lengths but no prominent axons (Fig. 7A, rows c and d), suggesting that both Vpr released from HIV-1-infected MDM and soluble rVpr induced abnormalities in neuronal development. As shown in Fig. 7A, row e, in slices cultured with rVpr plus z-DEVD-fmk, many EGFP-expressing cells had morphologies similar to those of cells in slices exposed to HIV-1-infected MDM or rVpr alone, suggesting that the effect of Vpr was not due to caspase-3-dependent apoptosis. In rVpr-treated slices cultured in the presence of both z-DEVD-fmk and UQ, more than one-third of the EGFP-expressing cells had a single elongated axon and were $NeuN^{high+}$, which is expressed specifically in the nuclei of mature neurons (Fig. 7B, row c), although most $EGFP^+$ cells had several minor neurites and were $NeuN^{dim+}$ in rVpr-treated slices cultured in the absence (Fig. 7B, row a) or the presence of z-DEVD-fmk (Fig. 7B, row b). Next, $EGFP^+$ cells were categorized into immature neurons or mature neurons by their morphologies and the expression of NeuN. $EGFP^+/NeuN^{dim+}$ cells, which have minor neurites but not extended axons, are classified as immature neurons, and $EGFP^+/NeuN^{high+}$ cells that have one elongated axon and several dendrites are classified as mature neurons. As shown in Fig. 7C, for EGFP-expressing mature neurons in rVpr-treated slices cultured in the presence of UQ or both z-DEVD-fmk and UQ, the percentages of EGFP-expressing mature neurons (33.80% ± 3.02% and 34.64% ± 1.83%, respectively) increased compared to those in rVpr-treated slices cultured with or without z-DEVD-fmk (18.48% ± 3.26% and 18.23% ± 1.78%, respectively). In addition, in HIV-CM-cocultured slices, the percentage of EGFP-expressing mature neurons increased in the presence of both z-DEVD-fmk and UQ (23.35% ± 3.42%) compared to that in slices cocultured with HIV-CM (8.65% ± 2.15%) (Fig. 7C). These results suggest that UQ has a protective effect on neuronal development in organotypic hippocampal slice cultures.

DISCUSSION

Neuronal damage can be caused by various viral or host factors, including viral products, excitotoxins, cytokines, and chemokines released from HIV-1-infected macrophages or microglial cells in HIV-1 encephalopathy (14, 29). Viral products such as HIV-1 gp120, Tat, and Vpr have been shown to be deleterious to neurons and to induce neuronal apoptosis (6, 9, 27, 30, 42). Recently, HIV-1-infected macrophages have been shown to affect neuronal development in a murine model (43), although the factors that affect neuronal development have not been identified and the mechanisms have not been clarified.

We found that HIV-1-infected macrophages produced an inhibitory factor(s) that induced the developmental arrest of neuronal progenitor cells, and we identified Vpr as one of the relevant viral factors (Fig. 1 and 2). Although several lines of evidence suggest that HIV-1 Vpr is a potentially toxic molecule that mediates cell death in mature neurons during HIV-1 infection (27, 42, 49), the influence of HIV-1 Vpr on neuronal development or neuronal plasticity has not been examined. Neuronal development can be divided into five morphological stages. First, cells form lamellipodia (stage 1). After several hours, the neurons form a number of immature neurites (stage 2). One of these minor neurites then begins to extend rapidly, becoming much longer than the other neurites (stage 3). This extended neurite becomes an axon. The other neurites then become mature dendrites (stage 4) and begin to establish dendritic components and to construct premature dendritic spines (stage 5) (4). It has been reported that it takes several days for plated neuronal progenitor cells to enter stage 4 (4). As we observed the cultured progenitors for 72 h, they were not investigated for progression beyond stage 3. We revealed that the majority of progenitor cells could extend primary neurites and proceed from stage 2 to stage 3 after 48 h in culture, although the majority of cells treated with both HIV-CM and recombinant Vpr protein could not extend primary neurites and proceed from stage 2 to stage 3 (Fig. 1 and 2), suggesting that Vpr is the key protein that had affected neuronal developmental arrest and caused the inhibition of axon formation in HIV-1-infected MDM. Although the neuronal developmental arrest was suppressed by treatment with anti-Vpr antibody, the

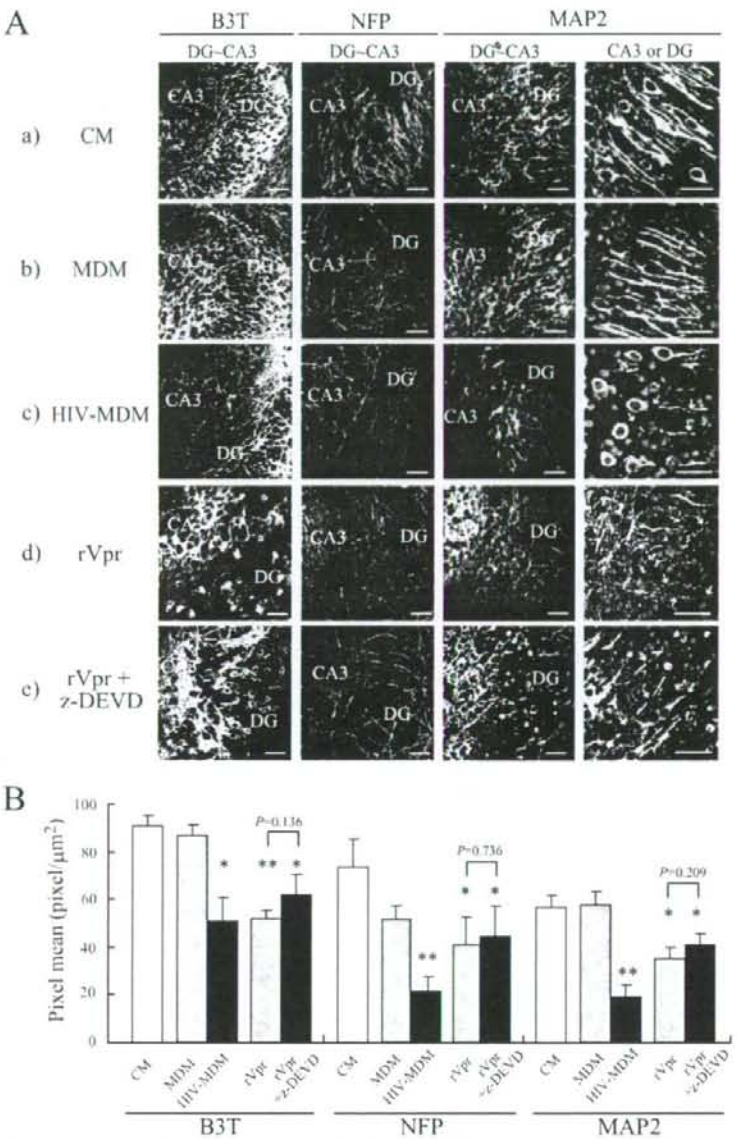

FIG. 6. Axonal disruption and atrophy of dendrites in organotypic hippocampal slices exposed to HIV-1-infected MDM or rVpr. (A) Organotypic hippocampal slices were cocultured alone (a) (CM), uninfected (b) (MDM) or HIV-1-infected MDM (c) (HIV-MDM), or rVpr alone (d) (rVpr) or in the presence of the caspase-3 inhibitor z-DEVD-fmk (e) (rVpr + z-DEVD). Slices were stained with antibodies against B3T, NFP, and MAP2 as described in Materials and Methods. Images were obtained using a 20× objective. Arrows indicate atrophy and the beading of dendrites. CA3, CA3 region of the hippocampus. Scale bars, 50 μm. (B) The mean pixels of the signal in representative areas of the B3T-, NFP-, and MAP2-stained samples shown in panel A were quantified. *, $P < 0.05$ compared to results from culture with CM or MDM (HIV-MDM) or CM (rVpr and rVpr + DEVD-fmk); **, $P < 0.01$ compared to results from culture with CM or MDM (HIV-MDM) or CM (rVpr and rVpr + z-DEVD).

recovery of neuronal development was not complete (Fig. 1E and F). In addition, soluble Vpr protein induced the inhibition of neuronal development in a manner similar to that of HIV-CM, although the effect on developmental retardation apparently was weaker than that of HIV-CM (Fig. 1 and 2). These results suggest that HIV-1-infected macrophages produce other viral proteins or cell-derived humoral factors that also affect neuronal development.

Vpr was found to induce an abnormality in mitochondrial transport at low concentrations through the suppression of

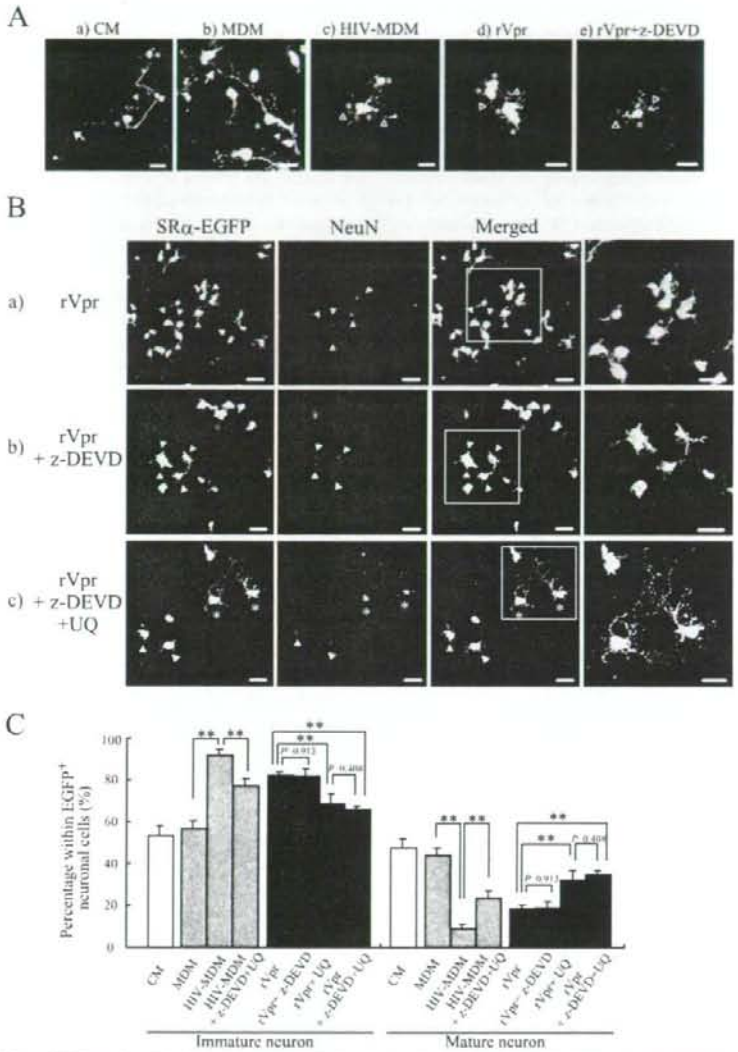

FIG. 7. Protective effect of UQ against Vpr-induced abnormality in neuronal development. (A) Endogenous precursor cells in the slices were labeled by an EGFP-expressing MLV vector, and slices were cocultured in C-CM (a), M-CM (b), HIV-CM (c), or rVpr in the absence (d) (rVpr) or in the presence of the caspase-3 inhibitor z-DEVD-fmk (e) (rVpr+z-DEVD). Arrows indicate axon-like processes. Filled arrowheads indicate dendrite-like processes, and opened arrowheads indicate neurite-like processes. Asterisks indicate neuronal cell bodies. Images were obtained using a 40× objective. Scale bars, 20 μm. (B) EGFP-expressing MLV vector-transduced slices were cultured in the presence of rVpr alone (a) (rVpr), rVpr and z-DEVD-fmk (b) (rVpr+z-DEVD), or rVpr, z-DEVD, and UQ (c) (rVpr+z-DEVD+UQ). Slices were stained with antibody against NeuN (red). Arrowheads indicate immature neurons, and asterisks indicate mature neurons. Rectangular regions were merged and enlarged. Images were obtained using a 40× objective. Scale bars, 20 μm. (C) MLV vector-transduced slices were cultured in CM, MDM, HIV-MDM, and HIV-MDM in the absence or presence of both UQ and z-DEVD-fmk (HIV-MDM+z-DEVD+UQ). Slices also were cultured with rVpr alone (rVpr), rVpr and z-DEVD-fmk (rVpr+z-DEVD), rVpr and UQ (rVpr+UQ), or both (rVpr+z-DEVD+UQ). In all experiments, 2.0 pM rVpr, 100 μM z-DEVD-fmk, and 100 μM UQ were used. $EGFP^+$ cells were classified as mature neurons ($EGFP^+$, $NeuN^{high+}$, and having one elongated axon) or immature neurons ($EGFP^+$, $NeuN^{dim+}$, and having a few neurites). **, $P < 0.01$.

ATP synthesis following mitochondrial membrane depolarization in neuronal progenitor cells (Fig. 3A and B). One of the major functions of mitochondria is to generate an intracellular source of ATP. Neuronal homeostasis is a highly dynamic process marked by an intense need for ATP, as ATP production is critical for the full functioning of motor proteins such as kinesin and dynein (10). As shown in Fig. 3C and D, the reduction of the ATP concentration in rVpr-treated neuronal

progenitor cells appeared to have a direct impact on the velocity of mitochondrial transport. Furthermore, we found significantly smaller amounts of mitochondria in the neurites (Fig. 3E and G), while the amount of mitochondria in whole cells seemed to be unaffected (Fig. 3F). Therefore, the developmental arrest and inhibition of neurite extension that we observed earlier in this study (Fig. 1 and 2) likely were caused by the retarded mitochondrial transport, as mitochondrial transport in neurites has been known to be important for neuronal development (10). Within the CNS, mitochondria are enriched in regions of high metabolic demand, especially in synapses (10, 15, 47). The necessity of mitochondrial transport in neuronal development and homeostasis is becoming clear (10). During neuronal cell differentiation from undifferentiated neuroblasts, cells acquire many neuronal processes. From these processes, axonal and dendritic branches form, and then synaptic connections assemble (10). These highly dynamic processes need large amounts of ATP to be produced at locations where it is needed. Therefore, the appropriate trafficking of mitochondria is a necessary task beginning in the earliest steps of neuronal development (10). To examine the physiological function of mitochondria, such as the maintenance of its membrane potential or ATP synthesis, some mitochondrion-targeted drugs (such as FCCP) previously have been used, and those drugs induced mitochondrial membrane depolarization and inhibited mitochondrial transportation within axons (46). The depolarization of the mitochondrial membrane potential and the inhibition of ATP synthesis caused retardation in mitochondrial transportation (10, 46). Therefore, the suppression of ATP synthesis following mitochondrial membrane depolarization by Vpr induced the retardation of mitochondrial transport into and within neurites, which may have arrested development.

Vpr is well known to induce apoptosis when a high concentration of Vpr is supplemented in culture or is exogenously expressed in cells (26, 27, 39, 41). It has been shown recently that Vpr induces cell cycle arrest following its binding to a large complex consisting of DDB1, Cul4A E3 ubiquitin ligase, and DDB1-Cul4A-associated factor 1 (8, 12, 13, 24, 33, 56, 59). Furthermore, synthetic Vpr peptides are found to directly bind to ANT, a component of the mPTP located on the inner mitochondrial membrane. As a result, a decrease of mitochondria membrane potential and the release of cytochrome *c* are thought to induce the intrinsic apoptosis pathway (25, 26, 48). As shown in Fig. 3A, high concentrations of rVpr (100 pM and 1.0 nM) induced the severe depression of $\Delta\Psi$m in progenitor cells, and the percentage of caspase-3-activated cells was significantly increased (Table 1). In contrast, although low concentrations of rVpr (2.0 and 10 pM) induced the moderate depression of $\Delta\Psi$m, no significant percentage of caspase-3-activated cells was detected. Furthermore, in 1.0 nM rVpr-treated cells, a large amount of cytochrome *c* was released into the cytosol, although cytochrome *c* was hardly released in cells treated with 2.0 pM rVpr (Fig. 4D). These results suggest that high concentrations of rVpr induce apoptosis via the release of cytochrome *c* from mitochondria through the severe reduction of $\Delta\Psi$m. In contrast, probably because a low concentration of rVpr induces a moderate reduction of $\Delta\Psi$m, the release of cytochrome *c* and apoptosis did not take place. However, the moderate reduction of $\Delta\Psi$m caused by treatment with a low concentration of rVpr is able to induce neuronal developmental arrest.

It has been reported that a Vpr peptide (aa 71 to 82) directly binds ANT in vitro, and the critical amino acids for the binding were mapped to three residues, R73, R77, and R80. Mitochondrial membrane depolarization was not caused by Vpr mutants that lacked those amino acids or carried their point mutations (25, 26). As shown in Fig. 3A, we showed that soluble Vpr induced mitochondrial membrane depolarization in neuronal progenitor cells in a dose-dependent manner. As suspected, a Vpr mutant that had mutations at the critical amino acids for its binding to ANT and that had been reported to be incapable of causing mitochondrial membrane depolarization was not able to induce any inhibitory effects on neuronal progenitor cells, including mitochondrial membrane depolarization and the inhibition of neuronal development. In addition, not only rVpr-WT but also the mutant incapable of causing depolarization (rVpr-R73, 77, 80A) were localized at the mitochondrial fraction in neuronal progenitor cells (Fig. 4D). These results suggest that Vpr localizes at the mitochondria and induces the inhibition of neuronal development through mitochondrial membrane depolarization because of the interaction with ANT. In contrast, although rVpr-R73, 77, 80A also localizes at the mitochondria, this mutant may not interact with ANT and induce neuronal developmental arrest.

The mPTP is a large conductance channel of solutes up to 1.5 kDa in size that spans the outer and inner mitochondrial membranes, and the mPTP is composed of the inner membrane ANT, the outer membrane voltage-dependent anion channel, and matrix cyclophilin D. The mPTP frequently is open under pathological conditions such as ATP depletion and mitochondrial membrane depolarization (10, 11). It is possible that the mPTP is opened because of an interaction between ANT and Vpr (25). It has been shown that UQ inhibits mitochondrial depolarization by closing the mPTP through direct interaction at the mPTP binding site (40, 58). Furthermore, recently UQ has been reported to have a protective effect on neurotoxicity in in vivo models of CNS diseases, including Parkinson's diseases, Huntington's disease, and amyotrophic lateral sclerosis, which all involve mitochondrial dysfunction (7). As shown in Fig. 5A, UQ was shown to restore the mitochondrial membrane potential and offer significant protection against rVpr, while the protection by a caspase-3 inhibitor, z-DEVD-fmk, was not statistically significant. In addition, ATP production and mitochondrion transportation was recovered by treatment with UQ but not z-DEVD-fmk (Fig. 5B and C). Even with the presence of z-DEVD-fmk, UQ was able to significantly restore $\Delta\Psi$m, ATP synthesis, and the velocity of mitochondrial transportation. This indicates that the inhibition of neuronal development observed in this study was caused independently of caspase-3-mediated apoptosis.

In HIV-1 encephalopathy, neurocognitive impairment is related to the loss of the synaptodendritic connection (1, 14). Our data demonstrated that not only inhibition of neuronal development but also axonal disruption and atrophy and beading of dendrites were induced by soluble Vpr protein and HIV-1-infected macrophages in organotypic hippocampal slice cultures (Fig. 6 and 7). It was reported that a significant amount of Vpr protein, as high as the nanogram-per-milliliter range, was detected in the CSF of AIDS patients (44). With

some circulating soluble Vpr protein in CNS, Vpr probably causes damage to both mature and immature neurons. Mature neurons may be damaged because of axonal disruption or synaptodendritic injury, and immature neurons may lose the ability to mature. In healthy adult brain, progenitor cells derived from DG of the hippocampus differentiate into mature neurons and are incorporated into the hippocampal circuitry. However, in HIV-1 encephalopathy patients, even when mature neurons are damaged, progenitor cells may not be able to properly differentiate because of the mitochondrial dysfunctions induced by Vpr. This might help the progression of hippocampus-dependent memory loss. Furthermore, we observed that low concentrations of soluble Vpr inhibited neuronal development and induced axonal disruption. It is possible that when low concentrations of Vpr infiltrate into the CNS, focal neuronal damage including axonal disruption and the inhibition of neuronal development are induced even if HIV-1-infected macrophages do not infiltrate into CNS tissues, and this may be a cause of mild neurocognitive disorder. In addition, in the pediatric patients who are affected by HIV-1-associated progressive encephalopathy, neurological dysfunction and developmental delays are seen (52). In the pediatric brain, there are large numbers of neuronal progenitor cells compared to the amount in the adult brain, and our data suggest that Vpr is one of the factors that induces neuronal developmental delay in pediatric patients. Neurotoxic viral and/or cell-derived factors besides Vpr possibly have the potential to induce neuronal developmental retardation, and the pathological process of HIV-1 encephalopathy may be caused by their added effects. To elucidate the pathology of HIV-1 encephalopathy, it is important to identify those factors and to clarify these complicated processes. Our findings suggest that Vpr is one of the important factors that spurs on the progression of HIV-1 encephalopathy.

ACKNOWLEDGMENTS

We thank Naoko Misawa and Chuanyi Nie for support in our study.

This work was supported by a Grant-in-Aid for Scientific Research on Priority Areas from the Ministry of Education, Culture, Sports, Sciences, and Technology of Japan and by grants for research on HIV-AIDS and health science from the Ministry of Health, Labor, and Welfare of Japan.

REFERENCES

1. **Adle-Biassette, H., F. Chretien, L. Wingertsmann, C. Hery, T. Ereau, F. Scaravilli, M. Tardieu, and F. Gray.** 1999. Neuronal apoptosis does not correlate with dementia in HIV infection but is related to microglial activation and axonal damage. Neuropathol. Appl. Neurobiol. **25:**123–133.
2. **Adle-Biassette, H., Y. Levy, M. Colombel, F. Poron, S. Natchev, C. Keohane, and F. Gray.** 1995. Neuronal apoptosis in HIV infection in adults. Neuropathol. Appl. Neurobiol. **21:**218–227.
3. **An, D. S., K. Morizono, Q. X. Li, S. H. Mao, S. Lu, and I. S. Chen.** 1999. An inducible human immunodeficiency virus type 1 (HIV-1) vector which effectively suppresses HIV-1 replication. J. Virol. **73:**7671–7677.
4. **Arimura, N., and K. Kaibuchi.** 2007. Neuronal polarity: from extracellular signals to intracellular mechanisms. Nat. Rev. Neurosci. **8:**194–205.
5. **Azuma, A., A. Matsuo, T. Suzuki, T. Kurosawa, X. Zhang, and Y. Aida.** 2006. Human immunodeficiency virus type 1 Vpr induces cell cycle arrest at the G_1 phase and apoptosis via disruption of mitochondrial function in rodent cells. Microbes Infect. **8:**670–679.
6. **Bachis, A., S. A. Aden, R. L. Nosheny, P. M. Andrews, and I. Mocchetti.** 2006. Axonal transport of human immunodeficiency virus type 1 envelope protein glycoprotein 120 is found in association with neuronal apoptosis. J. Neurosci. **26:**6771–6780.
7. **Beal, M. F.** 2004. Mitochondrial dysfunction and oxidative damage in Alzheimer's and Parkinson's diseases and coenzyme Q10 as a potential treatment. J. Bioenerg. Biomembr. **36:**381–386.
8. **Belzile, J. P., G. Duisit, N. Rougeau, J. Mercier, A. Finzi, and E. A. Cohen.** 2007. HIV-1 Vpr-mediated G2 arrest involves the DDB1-CUL4A(VPRBP) E3 ubiquitin ligase. PLoS Pathog. **3:**e85.
9. **Bruce-Keller, A. J., A. Chauhan, F. O. Dimayuga, J. Gee, J. N. Keller, and A. Nath.** 2003. Synaptic transport of human immunodeficiency virus-Tat protein causes neurotoxicity and gliosis in rat brain. J. Neurosci. **23:**8417–8422.
10. **Chang, D. T., and I. J. Reynolds.** 2006. Mitochondrial trafficking and morphology in healthy and injured neurons. Prog. Neurobiol. **80:**241–268.
11. **Crompton, M.** 1999. The mitochondrial permeability transition pore and its role in cell death. Biochem. J. **341:**233–249.
12. **Dehart, J. L., and V. Planelles.** 2007. HIV-1 Vpr links proteasomal degradation and checkpoint activation. J. Virol. doi:10.1128/JVI.01628–07.
13. **DeHart, J. L., E. S. Zimmerman, O. Ardon, C. M. Monteiro-Filho, E. R. Arganaraz, and V. Planelles.** 2007. HIV-1 Vpr activates the G2 checkpoint through manipulation of the ubiquitin proteasome system. Virol. J. **4:**57.
14. **Ellis, R., D. Langford, and E. Masliah.** 2007. HIV and antiretroviral therapy in the brain: neuronal injury and repair. Nat. Rev. Neurosci. **8:**33–44.
15. **Erecińska, M., and I. A. Silver.** 1994. Ions and energy in mammalian brain. Prog. Neurobiol. **43:**37–71.
16. **Eriksson, C., A. Bjorklund, and K. Wictorin.** 2003. Neuronal differentiation following transplantation of expanded mouse neurosphere cultures derived from different embryonic forebrain regions. Exp. Neurol. **184:**615–635.
17. **Gähwiler, B. H.** 1984. Development of the hippocampus in vitro: cell types, synapses and receptors. Neuroscience **11:**751–760.
18. **Gähwiler, B. H., M. Capogna, D. Debanne, R. A. McKinney, and S. M. Thompson.** 1997. Organotypic slice cultures: a technique has come of age. Trends Neurosci. **20:**471–477.
19. **Garden, G. A., S. L. Budd, E. Tsai, L. Hanson, M. Kaul, D. M. D'Emilia, R. M. Friedlander, J. Yuan, E. Masliah, and S. A. Lipton.** 2002. Caspase cascades in human immunodeficiency virus-associated neurodegeneration. J. Neurosci. **22:**4015–4024.
20. **González-Scarano, F., and J. Martin-Garcia.** 2005. The neuropathogenesis of AIDS. Nat. Rev. Immunol. **5:**69–81.
21. **Hollenbeck, P. J., and W. M. Saxton.** 2005. The axonal transport of mitochondria. J. Cell Sci. **118:**5411–5419.
22. **Horton, A. C., and M. D. Ehlers.** 2003. Neuronal polarity and trafficking. Neuron **40:**277–295.
23. **Hoshino, S., B. Sun, M. Konishi, M. Shimura, T. Segawa, Y. Hagiwara, Y. Koyanagi, A. Iwamoto, J. Mimaya, H. Terunuma, S. Kano, and Y. Ishizaka.** 2007. Vpr in plasma of HIV type 1-positive patients is correlated with the HIV type 1 RNA titers. AIDS Res. Hum. Retrovir. **23:**391–397.
24. **Hrecka, K., M. Gierszewska, S. Srivastava, L. Kozaczkiewicz, S. K. Swanson, L. Florens, M. P. Washburn, and J. Skowronski.** 2007. Lentiviral Vpr usurps Cul4-DDB1[VprBP] E3 ubiquitin ligase to modulate cell cycle. Proc. Natl. Acad. Sci. USA **104:**11778–11783.
25. **Jacotot, E., K. F. Ferri, C. El Hamel, C. Brenner, S. Druillennec, J. Hoebeke, P. Rustin, D. Metivier, C. Lenoir, M. Geuskens, H. L. Vieira, M. Loeffler, A. S. Belzacq, J. P. Briand, N. Zamzami, L. Edelman, Z. H. Xie, J. C. Reed, B. P. Roques, and G. Kroemer.** 2001. Control of mitochondrial membrane permeabilization by adenine nucleotide translocator interacting with HIV-1 viral protein R and Bcl-2. J. Exp. Med. **193:**509–519.
26. **Jacotot, E., L. Ravagnan, M. Loeffler, K. F. Ferri, H. L. Vieira, N. Zamzami, P. Costantini, S. Druillennec, J. Hoebeke, J. P. Briand, T. Irinopoulou, E. Daugas, S. A. Susin, D. Cointe, Z. H. Xie, J. C. Reed, B. P. Roques, and G. Kroemer.** 2000. The HIV-1 viral protein R induces apoptosis via a direct effect on the mitochondrial permeability transition pore. J. Exp. Med. **191:**33–46.
27. **Jones, G. J., N. L. Barsby, E. A. Cohen, J. Holden, K. Harris, P. Dickie, J. Jhamandas, and C. Power.** 2007. HIV-1 Vpr causes neuronal apoptosis and in vivo neurodegeneration. J. Neurosci. **27:**3703–3711.
28. **Kamada, M., R. Y. Li, M. Hashimoto, M. Kakuda, H. Okada, Y. Koyanagi, T. Ishizuka, and H. Yawo.** 2004. Intrinsic and spontaneous neurogenesis in the postnatal slice culture of rat hippocampus. Eur. J. Neurosci. **20:**2499–2508.
29. **Kaul, M., G. A. Garden, and S. A. Lipton.** 2001. Pathways to neuronal injury and apoptosis in HIV-associated dementia. Nature **410:**988–994.
30. **Kaul, M., and S. A. Lipton.** 1999. Chemokines and activated macrophages in HIV gp120-induced neuronal apoptosis. Proc. Natl. Acad. Sci. USA **96:**8212–8216.
31. **Koyanagi, Y., S. Miles, R. T. Mitsuyasu, J. E. Merrill, H. V. Vinters, and I. S. Chen.** 1987. Dual infection of the central nervous system by AIDS viruses with distinct cellular tropisms. Science **236:**819–822.
32. **Koyanagi, Y., W. A. O'Brien, J. Q. Zhao, D. W. Golde, J. C. Gasson, and I. S. Chen.** 1988. Cytokines alter production of HIV-1 from primary mononuclear phagocytes. Science **241:**1673–1675.
33. **Le Rouzic, E., N. Belaidouni, E. Estrabaud, M. Morel, J. C. Rain, C. Transy, and F. Margottin-Goguet.** 2007. HIV1 Vpr arrests the cell cycle by recruiting DCAF1/VprBP, a receptor of the Cul4-DDB1 ubiquitin ligase. Cell Cycle **6:**182–188.
34. **Levy, D. N., Y. Refaeli, R. R. MacGregor, and D. B. Weiner.** 1994. Serum Vpr

regulates productive infection and latency of human immunodeficiency virus type 1. Proc. Natl. Acad. Sci. USA **91:**10873–10877.
35. **Lledo, P. M., M. Alonso, and M. S. Grubb.** 2006. Adult neurogenesis and functional plasticity in neuronal circuits. Nat. Rev. Neurosci. **7:**179–193.
36. **Mattson, M. P.** 2007. Mitochondrial regulation of neuronal plasticity. Neurochem. Res. **32:**707–715.
37. **Mattson, M. P., and J. Partin.** 1999. Evidence for mitochondrial control of neuronal polarity. J. Neurosci. Res. **56:**8–20.
38. **Mizoguchi, I., Y. Ooe, S. Hoshino, M. Shimura, T. Kasahara, S. Kano, T. Ohta, F. Takaku, Y. Nakayama, and Y. Ishizaka.** 2005. Improved gene expression in resting macrophages using an oligopeptide derived from Vpr of human immunodeficiency virus type-1. Biochem. Biophys. Res. Commun. **338:**1499–1506.
39. **Muthumani, K., D. S. Hwang, B. M. Desai, D. Zhang, N. Dayes, D. R. Green, and D. B. Weiner.** 2002. HIV-1 Vpr induces apoptosis through caspase 9 in T cells and peripheral blood mononuclear cells. J. Biol. Chem. **277:**37820–37831.
40. **Papucci, L., N. Schiavone, E. Witort, M. Donnini, A. Lapucci, A. Tempestini, L. Formigli, S. Zecchi-Orlandini, G. Orlandini, G. Carella, R. Brancato, and S. Capaccioli.** 2003. Coenzyme Q10 prevents apoptosis by inhibiting mitochondrial depolarization independently of its free radical scavenging property. J. Biol. Chem. **278:**28220–28228.
41. **Patel, C. A., M. Mukhtar, and R. J. Pomerantz.** 2000. Human immunodeficiency virus type 1 Vpr induces apoptosis in human neuronal cells. J. Virol. **74:**9717–9726.
42. **Piller, S. C., P. Jans, P. W. Gage, and D. A. Jans.** 1998. Extracellular HIV-1 virus protein R causes a large inward current and cell death in cultured hippocampal neurons: implications for AIDS pathology. Proc. Natl. Acad. Sci. USA **95:**4595–4600.
43. **Polyektova, I., V. Meyer, L. Walters, X. Paez, and H. E. Gendelman.** 2005. Macrophage-induced inflammation affects hippocampal plasticity and neuronal development in a murine model of HIV-1 encephalitis. Glia **52:**344–353.
44. **Pomerantz, R. J.** 2004. Effects of HIV-1 Vpr on neuroinvasion and neuropathogenesis. DNA Cell Biol. **23:**227–238.
45. **Raineteau, O., L. Rietschin, G. Gradwohl, F. Guillemot, and B. H. Gahwiler.** 2004. Neurogenesis in hippocampal slice cultures. Mol. Cell Neurosci. **26:**241–250.
46. **Rintoul, G. L., A. J. Filiano, J. B. Brocard, G. J. Kress, and I. J. Reynolds.** 2003. Glutamate decreases mitochondrial size and movement in primary forebrain neurons. J. Neurosci. **23:**7881–7888.
47. **Rowland, K. C., N. K. Irby, and G. A. Spirou.** 2000. Specialized synapse-associated structures within the calyx of Held. J. Neurosci. **20:**9135–9144.
48. **Sabbah, E. N., S. Druillennec, N. Morellet, S. Bouaziz, G. Kroemer, and B. P. Roques.** 2006. Interaction between the HIV-1 protein Vpr and the adenine nucleotide translocator. Chem. Biol. Drug Des. **67:**145–154.
49. **Sabbah, E. N., and B. P. Roques.** 2005. Critical implication of the (70–96) domain of human immunodeficiency virus type 1 Vpr protein in apoptosis of primary rat cortical and striatal neurons. J. Neurovirol. **11:**489–502.
50. **Sacktor, N., M. P. McDermott, K. Marder, G. Schiffito, O. A. Selnes, J. C. McArthur, Y. Stern, S. Albert, D. Palumbo, K. Kieburtz, J. A. De Marcaida, B. Cohen, and L. Epstein.** 2002. HIV-associated cognitive impairment before and after the advent of combination therapy. J. Neurovirol. **8:**136–142.
51. **Schröfelbauer, B., Y. Hakata, and N. R. Landau.** 2007. HIV-1 Vpr function is mediated by interaction with the damage-specific DNA-binding protein DDB1. Proc. Natl. Acad. Sci. USA **104:**4130–4135.
52. **Schwartz, L., and E. O. Major.** 2006. Neural progenitors and HIV-1-associated central nervous system disease in adults and children. Curr. HIV Res. **4:**319–327.
53. **Shors, T. J., G. Miesegaes, A. Beylin, M. Zhao, T. Rydel, and E. Gould.** 2001. Neurogenesis in the adult is involved in the formation of trace memories. Nature **410:**372–376.
54. **Tachiwana, H., M. Shimura, C. Nakai-Murakami, K. Tokunaga, Y. Takizawa, T. Sata, H. Kurumizaka, and Y. Ishizaka.** 2006. HIV-1 Vpr induces DNA double-strand breaks. Cancer Res. **66:**627–631.
55. **Taguchi, T., M. Shimura, Y. Osawa, Y. Suzuki, I. Mizoguchi, K. Niino, F. Takaku, and Y. Ishizaka.** 2004. Nuclear trafficking of macromolecules by an oligopeptide derived from Vpr of human immunodeficiency virus type-1. Biochem. Biophys. Res. Commun. **320:**18–26.
56. **Tan, L., E. Ehrlich, and X. F. Yu.** 2007. DDB1 and Cul4A are required for human immunodeficiency virus type 1 Vpr-induced G_2 arrest. J. Virol. **81:**10822–10830.
57. **van Praag, H., A. F. Schinder, B. R. Christie, N. Toni, T. D. Palmer, and F. H. Gage.** 2002. Functional neurogenesis in the adult hippocampus. Nature **415:**1030–1034.
58. **Walter, L., V. Nogueira, X. Leverve, M. P. Heitz, P. Bernardi, and E. Fontaine.** 2000. Three classes of ubiquinone analogs regulate the mitochondrial permeability transition pore through a common site. J. Biol. Chem. **275:**29521–29527.
59. **Wen, X., K. M. Duus, T. D. Friedrich, and C. M. de Noronha.** 2007. The HIV1 protein Vpr acts to promote G2 cell cycle arrest by engaging a DDB1 and Cullin4A-containing ubiquitin ligase complex using VprBP/DCAF1 as an adaptor. J. Biol. Chem. **282:**27046–27057.

ELSEVIER

INSTITUT PASTEUR

Microbes and Infection xx (2009) 1–7

www.elsevier.com/locate/micinf

Original article

Activation of HIV-1 Gag-specific CD8$^+$ T cells by yeast-derived VLP-pulsed dendritic cells is influenced by the level of mannose on the VLP antigen

Fuminori Mizukoshi [a], Takuya Yamamoto [a], Yu-ya Mitsuki [a], Kazutaka Terahara [a], Ai Kawana-Tachikawa [b], Kazuo Kobayashi [a], Aikichi Iwamoto [b], Yuko Morikawa [c], Yasuko Tsunetsugu-Yokota [a,*]

[a] *Department of Immunology, National Institute of Infectious Diseases, Toyama 1-23-1 Shinjuku-ku, Tokyo, Japan*
[b] *Department of Infectious Diseases, Institute of Medical Science, University of Tokyo, Shirokanedai 4-6-1, Minato-ku, Tokyo, Japan*
[c] *Kitasato Institute for Life Sciences and Graduate School for Infection Control, Kitasato University, Shirokane 5-9-1, Minato-ku, Tokyo, Japan*

Received 3 October 2008; accepted 12 November 2008

Abstract

Dendritic cells (DCs) are professional antigen-presenting cells that possess a unique capacity to cross-present exogenous antigens efficiently to CD8$^+$ T cells. We previously demonstrated that monocyte-derived DCs (MDDCs) pulsed with yeast-derived HIV-1 Gag virus-like particles (VLPs) were able to activate Gag-specific CD8$^+$ T cells from HIV-1-infected individuals. Yeast VLPs are abundantly mannosylated (high-mannose type: HmVLPs) and are highly immunogenic. Because lectin receptors are shown to negatively regulate Th1 responses, we investigated the relationship between VLP mannosylation level and MDDC cross-presentation activity. Poorly mannosylated VLPs (low-mannose type: LmVLPs) were prepared using a yeast mnn9 mutant strain that lacks a core mannosylation enzyme. We found that MDDCs pulsed with LmVLPs activated Gag-specific T cells more strongly than those pulsed with HmVLPs. However, MDDCs showed similar antigen uptake and intracellular transport of both types of VLPs. Interestingly, LmVLPs induced IL-12 production slightly more than HmVLPs (yet statistically significant). Furthermore, the level of LPS-induced IL-10 production was enhanced by pulsing with HmVLPs, but not with LmVLPs. These results indicate that lectin receptors recognizing mannose may influence the Th1/Th2 balance of the immune response, resulting in reduced efficiency of CD8$^+$ T cell activation by a heavily mannosylated antigen presented by DCs.

Keywords: Antigen presentation; Mannosylation; AIDS

1. Introduction

Dendritic cells (DCs) are professional antigen-presenting cells that play a pivotal role in the immune system by acting as "sentinel cells" [1]. DC-based immunotherapy has been developed to treat a variety of diseases, including cancer [2,3], autoimmune diseases [4], transplant rejection [5], allergic diseases [6], and infectious diseases [7]. Previous studies of human immunodeficiency virus (HIV) and simian immunodeficiency virus (SIV) infections demonstrated that monocyte-derived DCs (MDDCs) pulsed with inactivated viruses enhanced both cellular and humoral immune responses [8,9]. However, the efficacies of DC-based immunotherapy for clinical applications have been inconsistent, probably because of the different protocols for cultivating and maturating the DCs, for the selection and loading of antigens, and for the administration, route, dose, and frequency of the therapy.

* Corresponding author: Tel.: +81 3 5285 1111x2133; fax: +81 3 5285 1150 or 1156.
E-mail address: yyokota@nih.go.jp (Y. Tsunetsugu-Yokota).

1286-4579/$ - see front matter Crown Copyright © 2008 Published by Elsevier Masson SAS. All rights reserved.
doi:10.1016/j.micinf.2008.11.004

Please cite this article in press as: F. Mizukoshi et al., Activation of HIV-1 Gag-specific CD8$^+$ T cells by yeast-derived VLP-pulsed dendritic cells is influenced by the level of mannose on the VLP antigen, Microb Infect (2009), doi:10.1016/j.micinf.2008.11.004

Acquired immune deficiency syndrome (AIDS), which is caused by HIV infection, is an enormous public health threat worldwide. The development of highly active anti-retroviral therapy (HAART) has markedly improved treatment of HIV-infected individuals and has significantly reduced HIV-associated mortality [10]. However, HAART cannot completely eradicate HIV [11]. Therefore, a novel strategy is required for treating HIV infections.

In terms of the host immune response against HIV, antigen-specific $CD8^+$ cytotoxic T lymphocytes (CTLs) are known to be important in suppressing HIV replication [12]. Therefore, CTL-inducible vaccines have been developed, most of them virus-based [13]. We previously showed that DCs pulsed with yeast-derived HIV-1 Gag virus-like particles (VLPs) activated Gag-specific T cells *in vitro* [14]. Because VLPs are neither infectious nor replicative, and also can be easily produced on a large scale, a VLP-based vaccine is an excellent candidate for a vaccine based on cross-presentation.

Highly glycosylated antigens have strong immunogenicity, whether expressed by yeast or using a baculoviral system. For example, mannosylation of antigens augments antigen-specific T cell responses [15,16]. However, recent studies revealed that the stimulation of lectin receptors on DCs induced interleukin (IL)-10 production, resulting in a shift in immune regulation towards Th2 dominance [17–19]. Thus, the influence of carbohydrate chains on the immune response is a concern for novel vaccine developments.

We postulated that the cross-presentation activity of DC is influenced by the degree of antigen mannosylation. In this study, we compared the antigenicity of abundantly mannosylated VLPs derived from a wild-type yeast to that of poorly mannosylated VLPs derived from a yeast mnn9 mutant lacking mannosylating enzyme.

2. Materials and methods

2.1. Preparation of cells

Fresh peripheral blood mononuclear cells (PBMCs) were obtained from healthy donors by Ficoll density gradient centrifugation. $CD14^+$ cells were positively isolated from PBMCs using a MACS system (Miltenyi Biotech, Bergisch Gladbach, Germany) according to the manufacturer's protocol. We generated immature MDDCs using 10 ng/ml human granulocyte-macrophage colony-stimulating factor and 20 ng/ml IL-4 as previously described [14]. These blood samples were collected with written informed consent under the approval of the ethical committee in National Institute of Infectious Diseases (NIID).

A Gag28 peptide (p17:KYKLKHIVW)-specific CTL line was established from PBMCs of HIV-1-infected individuals carrying HLA-A*2402 as previously described [20]. The studies utilizing PBMCs of HIV-infected patients were approved by the ethical committees in NIID and the Institute of Medical Science (University of Tokyo), and PBMCs were collected with written informed consent.

2.2. Production and purification of yeast-derived HIV-1 Gag VLPs

Wild-type yeast-derived VLPs from HIV-1 Gag, VLPs fused with green fluorescent protein (EGFP) and control culture supernatant (CS) were produced as described previously [14,21]. The mutant *S. cerevisiae* mnn9 strain [22] was used to produce low mannose-type VLPs. Standard purification and sucrose density gradient analysis of Gag VLPs was performed as described previously [23]. Purified VLPs were obtained by fractionation of the gradients. For comparison, *Spodoptera frugiperda* (*Sf*9) cells were infected with recombinant *Autographa californica* nuclear polyhedrosis viruses (baculoviruses) containing the full-length HIV-1 *gag* gene [23]. Purified Gag VLPs were quantitated by Coomassie brilliant blue staining. Total yeast protein was quantified by Bradford's method [21].

2.3. Quantitative analysis of mannose on the VLPs with dot blot technique

The samples were diluted with PBS and applied to a nitrocellulose membrane (0.45 μm pore size; GE Osmonics Labstore, Minnetonka, MA) using BioDot SF microfiltration apparatus (BioRad, Hercules, CA) according to the manufacturer's instructions. The membrane was soaked three times in blocking buffer (10 mM Tris–HCl pH 7.4, 0.15 M NaCl, 0.05% Tween20) for 10 min at room temperature (RT), then reacted with the biotinylated ConA (EY Laboratories, Inc., San Mateo, CA) (10 μg/ml in blocking buffer) for 90 min. After washing three times with blocking buffer, the membrane was incubated for 30 min at RT with horseradish peroxidase (HRP)-conjugated streptavidin (Boehringer-Roche, Basel, Switzerland) (1:5000 dilution). The SuperSignal West Dura kit (Pierce, Rockford, IL) was used for detection and the signal was analyzed by LAS-3000 (Fujifilm, Tokyo, Japan). The luminescence intensity of each dot was measured using Image Gauge densitometry software (version 4.0; Fujifilm).

2.4. Endocytosis assay

Immature MDDCs were incubated with various concentrations of CS or high- or low-mannose type VLP-EGFP at 37 °C for 3 h. These cells were washed extensively with flow cytometry (FCM) buffer (2% v/v fetal bovine serum and 50 μg/ml sodium azide in PBS), and resuspended in FCM buffer containing propidium iodide. The uptake of VLP-EGFP was quantified by measuring the fluorescence intensity using FACScalibur and CellQuest software (Becton Dickinson, Labware, NJ). For the receptor blocking assay, immature MDDCs were pre-cultured for 30 min in the presence of mAb against dendritic cell-specific intracellular adhesion molecule-3-grabbing nonintegrin (DC-SIGN) (10 μg/ml; eBioscience, San Diego, CA), mannose receptor (MR) mAb (10 μg/ml; BD Bioscience, Flanklin Lakes, NJ), mannan (2 mg/ml; Sigma–Aldrich) or isotype control IgG_{2a} (10 μg/ml; eBioscience), then pulsed with VLPs (10 μg/ml) or fluorescein-isothiocyanate

Please cite this article in press as: F. Mizukoshi et al., Activation of HIV-1 Gag-specific $CD8^+$ T cells by yeast-derived VLP-pulsed dendritic cells is influenced by the level of mannose on the VLP antigen, Microb Infect (2009), doi:10.1016/j.micinf.2008.11.004

(FITC)-conjugated mannosylated BSA (man-BSA; Sigma–Aldrich) (100 μg/ml).

2.5. Subcellular fractionation and Western blotting analysis

Immature MDDCs cultured with 40 μg/ml of high- or low-mannose type VLPs were washed with PBS and then fractionated into cytosol and membrane/organelle fractions using ProteoExtract subcellular proteome extraction kit (Calbiochem, Darmstadt, Germany).

For Western blotting, cells or subcellular fractions were resuspended in lysis buffer (10 mM Tris–HCl pH 7.4, 150 mM NaCl, 1% sodium deoxycholate, 1% Triton X-100, 0.1% sodium dodecyl sulfate, 357.5 mM 2-mercaptoethanol). The lysate, containing 2×10^5 cells, was analyzed by 12.5% SDS-PAGE and electrophoretically transferred to a PVDF transfer membrane (Amersham Biosciences, Buckinghamshire, UK). Non-specific binding was blocked with washing buffer (10 mM Tris–HCl, 150 mM NaCl, 0.05% Tween 20) containing 3% skim milk for 30 min at RT. After washing, the membrane was stained for 1 h at RT either with the anti-Calpain mAb (Calbiochem) as a cytosolic marker or anti-gastrin-releasing peptide (GRP) 78 mAb (BD Bioscience) as a membrane/organelle marker. Subsequently, the membrane was incubated with biotin-conjugated anti-mouse IgG for 1 h at RT, followed by streptavidin-conjugated HRP (Boehringer-Roche) for 30 min at RT. Gag p24 was detected by incubation with HRP-conjugated anti-HIV Gag mAbs (clone 10B5; kindly provided by T. Sata, Department of Pathology, NIID, Tokyo, Japan) [24] for 1 h at RT. The immunoreactive bands were detected with SuperSignal West Dura kit and visualized by Lumino analyzer LAS-3000.

2.6. Detection of cytokines

To detect IFN-γ production, an enzyme-linked immunospot (ELISPOT) assay was carried out as previously described [14]. The culture supernatant was collected and the level of cytokines was measured with the cytometric beads array kit (BD Bioscience) according to the manufacturer's protocol.

3. Results

3.1. Characterization of VLPs generated from yeast mutant mnn9

To determine whether the level of antigen mannosylation can modulate the immune response, we generated VLPs from wild-type yeast and from the mannosyltransferase mutant mnn9. The mnn mutants are mostly defective in polymerization enzymes related to the synthesis of the outer chain portion of N-linked oligosaccharides, and the mnn9 strain is defective in the core enzyme for glycosylation [25]. The wild-type yeast-derived VLPs are heavily mannosylated and are designated as high-mannose type VLPs (HmVLPs); in contrast, mnn9 mutants produce poorly mannosylated VLPs (low-mannose type VLPs: LmVLPs). The mannosylation level of LmVLPs is considered to be more similar to the level of mannose on mammalian mannoproteins than that of HmVLPs.

Using sucrose density gradient analysis, HmVLPs were recovered mainly at the density of 1.210 g/ml (Fig. 1A, upper panel), while the major peak density of LmVLPs was at 1.196 g/ml (Fig. 1A, middle panel) and the major peak of baculovirus-based VLPs was at 1.180 g/ml (Fig. 1A, lower panel). Thus, the LmVLPs are smaller in size than HmVLPs, probably due to the lower degree of mannosylation.

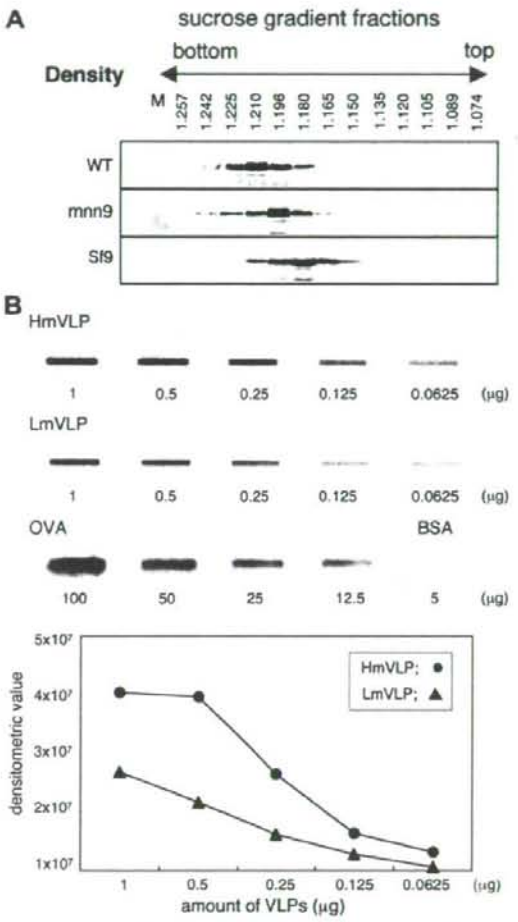

Fig. 1. Characterization of yeast VLPs. (A) Sucrose density gradient fractions were analyzed by Western blotting using anti-Gag mAbs. (Upper panel) HmVLPs derived from wild-type *S. cerevisiae* (WT). (Middle panel) LmVLPs derived from mnn9 mutant strain (mnn9). (Lower panel) VLPs derived from Sf9. 40 μg of VLPs were applied per assay, respectively. (B) Lectin staining was carried out on using biotinylated ConA and HRP-conjugated avidin. The number is indicative of the volume of sample applied per slot. The densitometric value of HmVLPs (filled circle) or LmVLPs (filled triangle) was measured by the computerization.

Please cite this article in press as: F. Mizukoshi et al., Activation of HIV-1 Gag-specific CD8+ T cells by yeast-derived VLP-pulsed dendritic cells is influenced by the level of mannose on the VLP antigen, Microb Infect (2009), doi:10.1016/j.micinf.2008.11.004

We next estimated the level of the mannosylation on these VLPs using lectin blot. In comparison with the LmVLPs generated from the mnn9 mutants, HmVLPs generated from a wild-type yeast strain clearly showed higher levels of mannose (Fig. 1B). As control, no mannose was detected in native BSA, while OVA was highly mannosylated. These results indicate that LmVLPs and HmVLPs differ in their mannose glycosylation levels.

3.2. The effect of uptake and intracellular dynamics of HmVLPs and LmVLPs

We first studied the internalization efficiency of EGFP-fused VLPs by MDDCs. We titrated the uptake of these VLPs at various concentrations (5–20 μg/ml). Both VLPs were taken up by MDDCs in a dose-dependent manner (Fig. 2A, upper panels), although the uptake of HmVLP was slightly better than that of LmVLP at 5 μg/ml.

In order to understand the mechanism of uptake of these VLPs by MDDCs, we carried out the blocking experiment. The uptake of these HmVLP and LmVLP at 10 μg/ml was strongly inhibited by mannan, but neither by anti-MR nor by anti-DC-SIGN mAbs (Fig. 2A, lowest panels). In contrast, the uptake of a high dose of man-BSA was remarkably inhibited by the same concentration of anti-MR, but not by anti-DC-SIGN mAb. Therefore, MDDCs are able to take up these VLPs at a similar level, probably by the mannose-mediated mechanism, but neither via DC-SIGN nor MR.

For cross-presentation of VLPs, the antigens incorporated in MDDCs have to be transported into the cytosol and processed by the proteasomes. To test whether the intracellular transport of VLPs is influenced by their level of mannosylation, the MDDCs were pulsed for 1 or 6 h with the

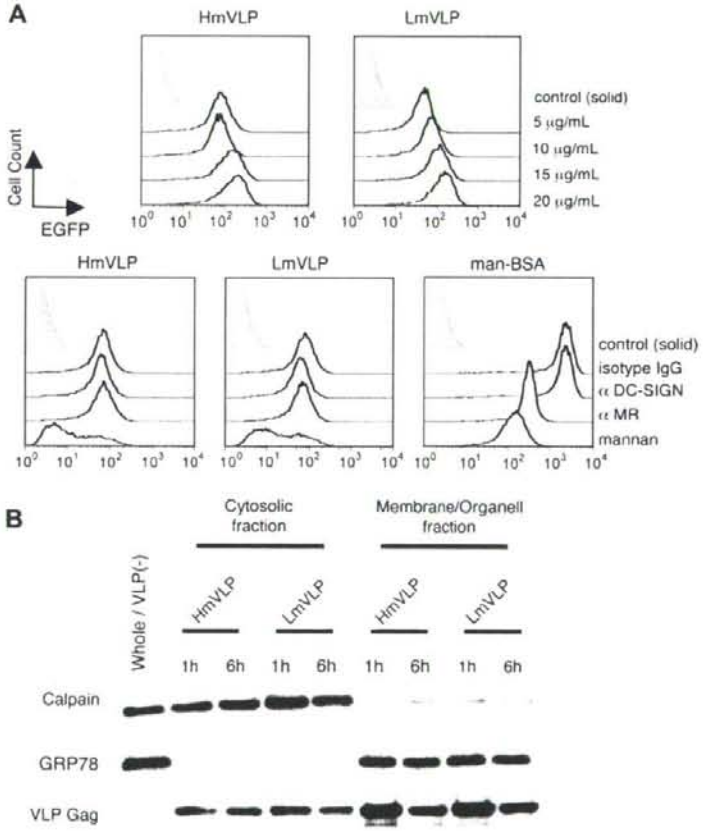

Fig. 2. Uptake and localization of yeast VLPs by DCs. (A) Immature MDDCs (5×10^4 cells/50 μl) were incubated with HmVLP-EGFP or LmVLP-EGFP (upper panel, indicated concentrations; lower panel, 10 μg/ml) for 3 h, analyzed by flow cytometry. Moreover, MDDCs were pre-incubated for 30 min with indicated antibodies (10 μg/ml) or mannan (2 mg/ml), and pulsed with HmVLP-EGFP or LmVLP-EGFP (10 μg/ml), mannosylated BSA (100 μg/ml) as a control (lower panel). The background signal is shown as a shadow. (B) Immature MDDCs (1×10^6 cells/200 μl) were incubated with 40 μg/ml yeast HmVLPs, LmVLPs or CS for 1 or 6 h, and fractionated. Whole cell lysate [Whole/VLP(−)] and cytosolic and membrane/organelle fractions were analyzed by Western blotting using antibodies against the cytosolic marker Calpain, the membrane marker GFP78, and VLP Gag.

Please cite this article in press as: F. Mizukoshi et al., Activation of HIV-1 Gag-specific CD8+ T cells by yeast-derived VLP-pulsed dendritic cells is influenced by the level of mannose on the VLP antigen, Microb Infect (2009), doi:10.1016/j.micinf.2008.11.004

VLPs at a high concentration (40 μg/ml) to obtain a strong signal, and fractionated. The level of HIV-1 Gag protein in the cytosolic and membrane/organelle fractions was analyzed by Western blot (Fig. 2B). As control, the calpain was detected mainly on the cytosolic fraction, whereas GRP78 was detected exclusively on the membrane/organelle fraction. There was no clear difference in the amount of Gag protein present in the cytosolic fractions in MDDCs pulsed with HmVLPs versus LmVLPs, as well as in the membrane/organelle fraction. We concluded that the mannosylation level of VLPs does not affect the internalization or the intracellular amount of Gag antigens in MDDCs.

3.3. LmVLPs are more efficiently cross-presented than HmVLPs for CD8$^+$ T cell (CTLs) activation by MDDCs

We next tested the efficiency of these VLPs on CTL activation by MDDC-mediated cross-presentation. We utilized HIV-1 Gag28 peptide-specific CTL lines established from HLA-A24$^+$ HIV-infected patients as an indicator cell for cross-presentation efficiency. Frozen HLA-A24$^+$ healthy donor-derived MDDCs were pulsed either with 10 μg/ml of HmVLPs or LmVLPs, cocultured with Gag-specific CTL lines for 40 h, and analyzed by IFN-γ ELISPOT.

For this experiment, three independent CTL lines (CTL #9, #21, and #31) were cocultured with VLP-pulsed MDDCs derived from two donors each (Fig. 3). Despite the MDDCs' donor variation, LmVLP-pulsed MDDCs were able to activate higher numbers of Gag28-specific CTL lines compared to HmVLP-pulsed MDDCs in four of six MDDCs. Thus, our results suggest that the level of mannose on antigens can modulate the cross-presenting activity of VLPs by MDDCs.

3.4. Cytokine production by MDDCs after uptake of VLPs is influenced by the level of VLP mannosylation

For effective induction of CTL activity, it is important to polarize DCs toward Th1-type cytokine secretion during the DC–T cell interaction. We previously showed that MDDCs stimulated with yeast VLPs produced a higher level of IL-12 than those stimulated with LPS, while IL-10 production is limited [14]. We therefore measured cytokine production by 10 μg/ml of HmVLP- or LmVLP-pulsed MDDCs from eight healthy donors. Two patterns of IL-12 production were identified: IL-12 responders ($n = 4$), and IL-12 non-responders ($n = 4$) (Fig. 4).

In the case of the IL-12 responders, IL-12 production induced by LmVLPs tended to be higher than that by HmVLP (Fig. 4A), though the difference was not statistically significant. In contrast, the level of IL-10 production was very low in these donors (data not shown).

In IL-12 non-responders, both IL-12 and IL-10 production by LmVLP- or HmVLP-pulsed MDDCs were consistently low (data not shown). When we stimulated the MDDCs from these donors with LPS, the production of IL-10, but not IL-12, was increased, and the LPS-induced IL-10 production

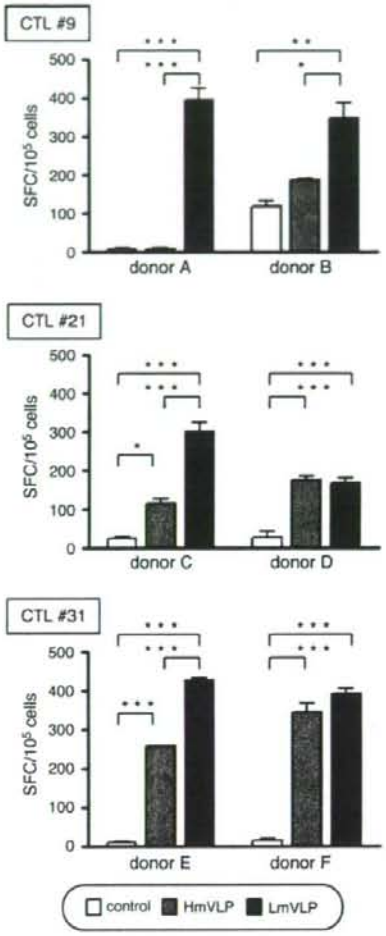

Fig. 3. The influence of yeast VLPs on HIV Gag-specific CD8$^+$ T cell activation. Immature MDDCs were pulsed overnight with 10 μg/ml HmVLPs (gray bar), LmVLPs (filled bar), or CS (open bar). Next day, MDDCs (1×10^4 cells per well) were mixed with MHC class I-matched allogenic CTL clones ($1–2 \times 10^4$ per well). Two days after cocultivation, the number of IFN-γ-producing cells was determined by ELISPOT analysis. The longitudinal axis shows the analysis spot forming cells (SFC) producing IFN-γ per 10^5 cells. Results are presented as the means + SEM. $^*P < 0.05$; $^{**}P < 0.01$; $^{***}P < 0.001$, compared between two groups; one-way ANOVA followed by Bonferroni's t-test ($n = 3$).

was upregulated further in the presence of HmVLPs, while it was not true for LmVLPs (Fig. 4B). The level of IL-12 production remained undetectable or low even after stimulation with LPS plus HmVLPs or LPS plus LmVLPs (data not shown). The production of other cytokines (including IL-1, IL-6, IL-8, and TNF-alpha) was very low or showed little difference in response to HmVLPs and LmVLPs. These results suggest that a high level of mannosylation modulates the cytokine production by MDDCs toward a Th2-type response.

Please cite this article in press as: F. Mizukoshi et al., Activation of HIV-1 Gag-specific CD8$^+$ T cells by yeast-derived VLP-pulsed dendritic cells is influenced by the level of mannose on the VLP antigen, Microb Infect (2009), doi:10.1016/j.micinf.2008.11.004

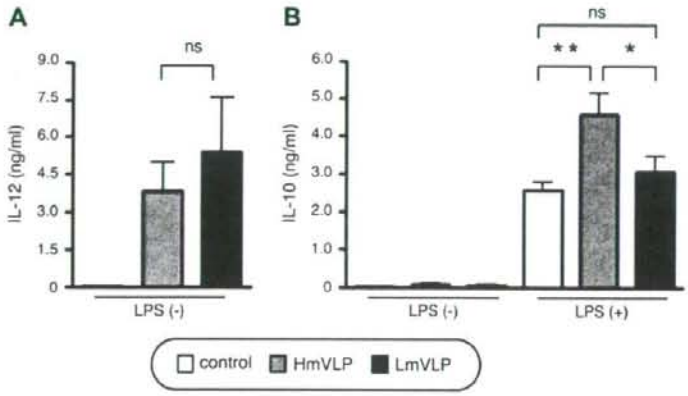

Fig. 4. The effect of yeast VLPs on cytokine production. (A) In the cases of IL-12 responders ($n = 4$), immature MDDCs (2×10^5 cells/200 μl) were incubated with 20 μg/ml HmVLPs (gray bar), LmVLPs (filled bar), or CS (open bar) for 24 h. (B) The MDDCs (2×10^5 cells/200 μl) of IL-12 non-responders ($n = 4$) were incubated with 20 μg/ml HmVLPs (gray bar), LmVLPs (filled bar), or CS (open bar) with or without 100 ng/ml LPS for 24 h. The cytokines produced by these cells were analyzed. Results are presented as the means + SEM. $^*P < 0.05$; $^{**}P < 0.01$; ns, not significant, compared between two groups; one-way ANOVA followed by Bonferroni's *t*-test ($n = 4$, respectively).

4. Discussion

Antigens expressed by yeast and insect cells contain abundant carbohydrate modifications and are perceived to be excellent vaccine antigens. Consistent with these observations, we previously demonstrated that MDDCs loaded with yeast-derived HIV-1 $p55^{gag}$ VLPs activated Gag-specific $CD8^+$ T cells in chronically-infected HIV patients [14]. Mannosylated antigens taken up by DCs are more efficiently presented to T cells than antigens internalized via fluid phase [15]. However, recent studies have indicated that excessive mannosylation leads to a Th2-dominant response or even suppresses the immune response via a signal from the lectin receptors [17–19]. Therefore, it is important to determine whether the level of mannosylation on VLPs positively or negatively affects the DC-based immune response.

The cell wall of *Saccharomyces cerevisae* is rich in mannoproteins. In this work, we used a yeast mnn9 mutant of the mannosyltransferase, which cannot synthesize completely glycosylated mannoproteins, and demonstrated that VLPs with much reduced mannose induced stronger CTL activation than more heavily mannosylated VLPs derived from wild-type yeast did. Because we used the same amount of Gag protein composed of these VLPs, the difference should be only at the level of glycosylation on VLPs. The efficiency of CTL activation by VLP-pulsed MDDCs was analyzed at 10–20 μg/ml concentration of VLPs. At this concentration, we detected no difference of uptake by FACS analysis. We speculate that the difference, if any, may be not at the level of uptake, but rather during antigen processing or loading to MHC class I. Although we failed to show the difference in the intracellular fate of these VLPs by the current technology, it is still possible that they are differently processed somewhere in the cytoplasm. In this context, it has been demonstrated previously that only a small amount (200 molecules) of peptide and MHC class I complex is enough to be recognized by CTLs [26]. Therefore, even a small difference in the antigen processing process may affect the efficiency of cross-presentation by DCs.

The balance of the Th1/Th2 immune response is influenced by elements such as host conditions and the antigen formulation [27]. LmVLPs induced IL-12 production slightly better than HmVLPs in some donors, whereas in those who do not produce a substantial level of IL-12, LPS-induced IL-10 production was increased by adding HmVLPs, but not by LmVLPs. A number of studies have demonstrated that cytokine production can be altered by the interaction of antigen with lectin receptors and/or toll-like receptors [17–19,28]. For example, Nigou et al. reported that the IL-12 production of DCs induced by LPS was negatively regulated by the engagement of an MR using mannose-capped lipoarabinomannans (the ManLAMs) of *Mycobacteria* [28]. Gringhuis et al. reported that stimulation of DC-SIGN by pathogens such as *Mycobacteria*, fungi, and viruses enhanced toll-like receptor signaling via Raf-1 kinase-dependent acetylation of the transcription factor NF-kB, resulting in strong augmentation of IL-10 mRNA expression by DCs [19]. Thus, stimulation of lectin receptors may preferentially induce IL-10 production in low IL-12 responders. We speculate that a mannosylation-dependent signal affects the Th1/Th2 balance by modulating the cytokine production of DCs, leading to the alternation of CTL activation.

In conclusion, a high level of mannosylation on an antigen may not necessarily be beneficial for CTL induction by DCs. The quantity of carbohydrate chain may alter the Th1/Th2 cytokine balance. DC-based immune therapy that aims to induce CTLs requires optimizing the antigen for the most effective clinical results. Further studies are required to develop the technology for modulating the antigenic property so that it can efficiently induce Th-1 type immune response.

Please cite this article in press as: F. Mizukoshi et al., Activation of HIV-1 Gag-specific $CD8^+$ T cells by yeast-derived VLP-pulsed dendritic cells is influenced by the level of mannose on the VLP antigen, Microb Infect (2009), doi:10.1016/j.micinf.2008.11.004

One possible technology may be the modification of the outer structure, amount and variation of sugars moieties on vaccine antigens.

Acknowledgments

We are grateful to T. Sata (Department of Pathology, NIID, Tokyo, Japan) for anti-HIV Gag mAbs (clone 10B5). We are indebted to T. Murakami (AIDS Research Center, NIID, Tokyo, Japan) for excellent technical advice on the subcellular fractionation experiment. This work was supported by a grant from the Ministry of Health, Labour, and Welfare of Japan. F. Mizukoshi receives support from the Japanese Foundation for AIDS Prevention.

References

[1] J. Banchereau, R.M. Steinman, Dendritic cells and the control of immunity, Nature 392 (1998) 245–252.
[2] J. Banchereau, A.K. Palucka, Dendritic cells as therapeutic vaccines against cancer, Nat. Rev. Immunol. 5 (2005) 296–306.
[3] C.G. Figdor, I.J. de Vries, W.J. Lesterhuis, C.J. Melief, Dendritic cell immunotherapy: mapping the way, Nat. Med. 10 (2004) 475–480.
[4] A.G. Thompson, R. Thomas, Induction of immune tolerance by dendritic cells: implications for preventative and therapeutic immunotherapy of autoimmune disease, Immunol. Cell Biol. 80 (2002) 509–519.
[5] T.E. Ichim, R. Zhong, W.P. Min, Prevention of allograft rejection by in vitro generated tolerogenic dendritic cells, Transpl. Immunol. 11 (2003) 295–306.
[6] H. Matsue, M. Kusuhara, K. Matsue, A. Takashima, Dendritic cell-based immunoregulatory strategies, Int. Arch. Allergy Immunol. 127 (2002) 251–258.
[7] J. Colino, C.M. Snapper, Dendritic cells, new tools for vaccination, Microbes Infect 5 (2003) 311–319.
[8] W. Lu, L.C. Arraes, W.T. Ferreira, J.M. Andrieu, Therapeutic dendritic-cell vaccine for chronic HIV-1 infection, Nat. Med. 10 (2004) 1359–1365.
[9] W. Lu, X. Wu, Y. Lu, W. Guo, J.M. Andrieu, Therapeutic dendritic-cell vaccine for simian AIDS, Nat. Med. 9 (2003) 27–32.
[10] R.J. Pomerantz, D.L. Horn, Twenty years of therapy for HIV-1 infection, Nat. Med. 9 (2003) 867–873.
[11] D. Finzi, J. Blankson, J.D. Siliciano, J.B. Margolick, K. Chadwick, T. Pierson, K. Smith, J. Lisziewicz, F. Lori, C. Flexner, T.C. Quinn, R.E. Chaisson, E. Rosenberg, B. Walker, S. Gange, J. Gallant, R.F. Siliciano, Latent infection of CD4+ T cells provides a mechanism for lifelong persistence of HIV-1, even in patients on effective combination therapy, Nat. Med. 5 (1999) 512–517.
[12] B.D. Walker, B.T. Korber, Immune control of HIV: the obstacles of HLA and viral diversity, Nat. Immunol. 2 (2001) 473–475.
[13] A. Duerr, J.N. Wasserheit, L. Corey, HIV vaccines: new frontiers in vaccine development, Clin. Infect. Dis. 43 (2006) 500–511.
[14] Y. Tsunetsugu-Yokota, Y. Morikawa, M. Isogai, A. Kawana-Tachikawa, T. Odawara, T. Nakamura, F. Grassi, B. Autran, A. Iwamoto, Yeast-derived human immunodeficiency virus type 1 p55(gag) virus-like particles activate dendritic cells (DCs) and induce perforin expression in Gag-specific CD8(+) T cells by cross-presentation of DCs, J. Virol. 77 (2003) 10250–10259.
[15] A.J. Engering, M. Cella, D. Fluitsma, M. Brockhaus, E.C. Hoefsmit, A. Lanzavecchia, J. Pieters, The mannose receptor functions as a high capacity and broad specificity antigen receptor in human dendritic cells, Eur. J. Immunol. 27 (1997) 2417–2425.
[16] M.C. Tan, A.M. Mommaas, J.W. Drijfhout, R. Jordens, J.J. Onderwater, D. Verwoerd, A.A. Mulder, A.N. van der Heiden, D. Scheidegger, L.C. Oomen, T.H. Ottenhoff, A. Tulp, J.J. Neefjes, F. Koning, Mannose receptor-mediated uptake of antigens strongly enhances HLA class II-restricted antigen presentation by cultured dendritic cells, Eur. J. Immunol. 27 (1997) 2426–2435.
[17] E. Caparros, P. Munoz, E. Sierra-Filardi, D. Serrano-Gomez, A. Puig-Kroger, J.L. Rodriguez-Fernandez, M. Mellado, J. Sancho, M. Zubiaur, A.L. Corbi, DC-SIGN ligation on dendritic cells results in ERK and PI3K activation and modulates cytokine production, Blood 107 (2006) 3950–3958.
[18] T.B. Geijtenbeek, S.J. Van Vliet, E.A. Koppel, M. Sanchez-Hernandez, C.M. Vandenbroucke-Grauls, B. Appelmelk, Y. Van Kooyk, *Mycobacteria* target DC-SIGN to suppress dendritic cell function, J. Exp. Med. 197 (2003) 7–17.
[19] S.I. Gringhuis, J. den Dunnen, M. Litjens, B. van Het Hof, Y. van Kooyk, T.B. Geijtenbeek, C-type lectin DC-SIGN modulates Toll-like receptor signaling via Raf-1 kinase-dependent acetylation of transcription factor NF-kappaB, Immunity 26 (2007) 605–616.
[20] A. Kawana-Tachikawa, M. Tomizawa, J. Nunoya, T. Shioda, A. Kato, E.E. Nakayama, T. Nakamura, Y. Nagai, A. Iwamoto, An efficient and versatile mammalian viral vector system for major histocompatibility complex class I/peptide complexes, J. Virol. 76 (2002) 11982–11988.
[21] S. Sakuragi, T. Goto, K. Sano, Y. Morikawa, HIV type 1 Gag virus-like particle budding from spheroplasts of Saccharomyces cerevisiae, Proc. Natl. Acad. Sci. USA 99 (2002) 7956–7961.
[22] C.E. Ballou, Isolation, characterization, and properties of *Saccharomyces cerevisiae* mnn mutants with nonconditional protein glycosylation defects, Methods Enzymol 185 (1990) 440–470.
[23] Y. Morikawa, S. Hinata, H. Tomoda, T. Goto, M. Nakai, C. Aizawa, H. Tanaka, S. Omura, Complete inhibition of human immunodeficiency virus Gag myristoylation is necessary for inhibition of particle budding, J. Biol. Chem. 271 (1996) 2868–2873.
[24] Y. Tsunetsugu-Yokota, K. Akagawa, H. Kimoto, K. Suzuki, M. Iwasaki, S. Yasuda, G. Hausser, C. Hultgren, A. Meyerhans, T. Takemori, Monocyte-derived cultured dendritic cells are susceptible to human immunodeficiency virus infection and transmit virus to resting T cells in the process of nominal antigen presentation, J. Virol. 69 (1995) 4544–4547.
[25] C.E. Ballou, Yeast cell wall and cell surface, in: J.N. Stranthern, E.W. Jones, J.R. Broach (Eds.), The Molecular Biology of the Yeast Saccharomyces, Metabolism and Gene Expression, Cold Spring Harbor Laboratory Press, Cold Spring Harbor, NY, 1982, pp. 335–360.
[26] E.R. Christinck, M.A. Luscher, B.H. Barber, D.B. Williams, Peptide binding to class I MHC on living cells and quantitation of complexes required for CTL lysis, Nature 352 (1991) 67–70.
[27] P. Kidd, Th1/Th2 balance: the hypothesis, its limitations, and implications for health and disease, Altern. Med. Rev. 8 (2003) 223–246.
[28] J. Nigou, C. Zelle-Rieser, M. Gilleron, M. Thurnher, G. Puzo, Mannosylated lipoarabinomannans inhibit IL-12 production by human dendritic cells: evidence for a negative signal delivered through the mannose receptor, J. Immunol. 166 (2001) 7477–7485.

Please cite this article in press as: F. Mizukoshi et al., Activation of HIV-1 Gag-specific CD8+ T cells by yeast-derived VLP-pulsed dendritic cells is influenced by the level of mannose on the VLP antigen, Microb Infect (2009), doi:10.1016/j.micinf.2008.11.004

Highly restricted TCR repertoire in the CD8$^+$ T-cell response against an HIV-1 epitope with a stereotypic amino acid substitution

Eriko Miyazaki[a,*], Ai Kawana-Tachikawa[a,*], Mariko Tomizawa[a], Jun-ichi Nunoya[a], Takashi Odawara[a], Takeshi Fujii[b], Yi Shi[d], George Fu Gao[d] and Aikichi Iwamoto[a,b,c]

Objective: In peripheral blood mononuclear cells (PBMCs) from HIV-1-positive patients, we sought to identify CD8$^+$ T-cell populations and the corresponding T-cell receptor (TCR) repertoires that react to an immunogenic cytotoxic T lymphocyte (CTL) epitope with or without an escape mutation.

Methods: PBMCs from HLA-A*2402(A24)-positive patients were stimulated with peptides representing a wild-type CTL epitope in the HIV-1 Nef protein [Nef138-10(wt)] or an escape mutant with a Y to F (Y139F) substitution at the second position [Nef138-10(2F)]. Cultured PBMCs were stained with peptide-major histocompatibility complex tetramers containing Nef138-10(wt) or Nef138-10(2F) sequences. After in-vitro stimulation of PBMCs with cognate peptides, the CD8$^+$ T-cell population was sorted into different fractions: positive only to the wild-type tetramer (wt-positive), positive only to the mutant tetramer (2F-positive), and positive to both wt-tetramers and mutant-tetramers (dual-positive). TCR repertoires of sorted epitope-specific CD8$^+$ T-cell populations were determined by sequencing.

Results: A 2F-positive population was rarely observed under our culture and staining conditions. The wt-positive CD8$^+$ T-cell populations had a diverse TCR repertoire, but the TCR repertoires in dual-positive CD8$^+$ populations were highly restricted. In the dual-positive CD8$^+$ T-cell populations, most clonotypes used the TRBV4-1 and TRBJ2-7 gene segments for the TCR β-chain and the TRAV8-3 and TRAJ40-1 for the TCR α-chain. The CDR3 region of the TCR β-chain showed little variation.

Conclusion: These results provide an example of restricted TCR repertoire in a specific CTL response against the escaping epitope. We speculate that impairment of antigen presentation in escaping viruses may underlie the restricted repertoire.

AIDS 2009, **23**:000–000

Keywords: CD8$^+$ T cells, HIV infection, human leukocyte antigen, T-cell epitope, T-cell receptor repertoire

Introduction

Cytotoxic T lymphocytes (CTLs) play a very important role in counteracting HIV-1 infection [1–3]. However, the hallmark of HIV-1 infection is the incomplete response of CTLs. It is crucial to understand the molecular mechanisms of antigen presentation and recognition in the context of immunopathogenesis of HIV-1.

[a]Division of Infectious Diseases, Advanced Clinical Research Center, [b]Department of Infectious Diseases and Applied Immunology, Research Hospital, [c]Research Center for Asian Infectious Diseases, The Institute of Medical Science, The University of Tokyo, Tokyo, Japan, and [d]Division of Molecular Immunology, Institute of Microbiology, Chinese Academy of Sciences, Beijing, China.

Correspondence to Aikichi Iwamoto, MD, Professor, Division of Infectious Diseases, Advanced Clinical Research Center, The Institute of Medical Science, The University of Tokyo, 4-6-1 Shirokanedai, Minato-ku, Tokyo 108-8639, Japan.

Tel: +81 3 5449 5359; fax: +81 3 6409 2008; e-mail: aikichi@ims.u-tokyo.ac.jp

* E. Miyazaki and A. Kawana-Tachikawa contributed equally to the writing of this article.

Received: 28 August 2008; revised: 12 November 2008; accepted: 25 November 2008.

DOI:10.1097/QAD.0b013e32832605e6

ISSN 0269-9370 © 2009 Wolters Kluwer Health | Lippincott Williams & Wilkins

CTLs use T-cell receptors (TCRs) to recognize peptide-major histocompatibility complex (MHC) (pMHC) complexes presented on the surface of the infected cells. Error-prone reverse transcription of HIV-1 can result in amino acid substitutions in the cognate peptides. Mutated viruses may acquire selective advantage against CTLs and become dominant escape variants [4,5]. Substitution of amino acid residues critical for binding to MHC molecules [6,7] or TCR recognition [8,9] can result in escape mutants. Even substitution of the amino acids flanking the cognate peptides can result in escape mutants by altering the peptide processing and decreasing the number of pMHC molecules that are recognized by CTLs [10–14].

Amino acid substitutions in the HIV-1 escape mutants may be stereotypic in different individuals sharing the same MHC haplotypes [12,15]. We previously reported that HIV-1 with a stereotypic substitution from Y [Nef138-10(wt)] to F [Nef138-10(2F)] at the second position in an immunodominant HLA-A*2402(A24)-restricted CTL epitope in the Nef protein (Nef138-10) has a strong selective advantage in A24-positive patients [12]. There is a high prevalence of A24 in the Japanese population, and unprotected sexual contact has transmitted the 2F substitution among A24-positive individuals throughout Japan. How HIV-1 with the Nef138-10(2F) substitution could have a selective advantage in A24-positive patients remains an enigma, as we detected vigorous $CD8^+$ positive T-cell ($CD8^+$) responses not only against Nef138-10(wt) but also against Nef138-10(2F) in PBMCs from A24-positive patients [12].

In this study to explore the effector side, we stimulated cultured $CD8^+$ T cells obtained from A24-positive, HIV-1-infected patients and stained them simultaneously with two A24 tetramers that presented either Nef138-10(wt) or Nef138-10(2F). We then sorted the epitope-specific $CD8^+$ T cells that recognized wild-type or 2F or both and analyzed the TCR repertoire.

Materials and methods

Study patients

We analyzed CTL response in peripheral blood mononuclear cells (PBMCs) from seven patients who were HIV-1-infected and HLA-A*2402 positive. patients were randomly selected among patients participating in an ongoing HIV-1-immunopathogenesis study at an HIV outpatient clinic affiliated with the Institute of Medical Science, the University of Tokyo. All but one of the seven subjects (S15) were antiretroviral therapy-naive. The study was approved by the internal review board of the Institute of the Medical Science of the University of Tokyo (No. 11-2), and all patients provided informed consent.

Cell media and study reagents

Culture media and supplements were purchased from Sigma (St Louis, Missouri, USA) except as otherwise noted. R(−) medium consisted of RPMI 1640 supplemented with 100 U/ml penicillin, 100 μg/ml streptomycin, 10 mmol/l 4-(2-hydroxyethyl)-1-piperazineethanesulfonic acid (HEPES) and 2 mmol/l L-glutamine. R10 medium was R(−) medium supplemented with 10% heat-inactivated fetal calf serum (FCS).

Synthetic peptides Nef138-10(wt) (RYPLTFGWCF), Nef138-10(2F) (RFPLTFGWCF) were purchased from Sigma-Genosys (Ishikari-shi, Hokkaido, Japan).

Enzyme-linked immunosorbent spot assay

Enzyme-linked immunosorbent spot (ELISPOT) assay was performed using freshly prepared PBMCs (5×10^4 cells) as previously described [16].

In-vitro stimulation with Nef138-10 peptides

PBMCs were divided into two aliquots and prepared for in-vitro stimulation with Nef138-10 peptides as previously described [17]. To prepare antigen-presenting cells, PBMCs of 5×10^5 patients were pulsed with 10 nmol/l Nef138-10(wt) or Nef138-10(2F) at 37°C for 1 h. Cells were washed twice with R10, then cultured in R10 with 1×10^6 fresh autologous PBMCs and 4×10^6 irradiated (3300 rads) PBMCs from healthy individuals. After 4 days, recombinant human IL-2 (rIL-2; Wako, Osaka, Japan) was added to 50 U/ml. The culture was continued for 2 weeks, with medium changed every 3–4 days (R10 with 50 U/ml rIL-2).

Preparation of major histocompatibility complex-class I tetramers presenting Nef138-10(wt) or Nef138-10(2F)

Soluble forms of pMHC molecules were produced in CV-1 cells using a Sendai virus (SeV) vector expression system and purified from the supernatant as described previously [18]. After affinity purification, pMHC molecules were biotinylated with BirA enzyme (Avidity, Aurora, Colorado, USA) and purified by gel filtration chromatography with Superdex 200 column (GE Healthcare, Piscataway, New Jersey, USA).

Biotinylated Nef138-10(wt)/HLA-A24 (Nef138-10(wt)/A24) or Nef138-10(2F)/HLA-A24 (Nef138-10(2F)/A24) complexes were tetramerized with allophycocyanin (APC)-labeled or phycoerythrin-labelled streptavidins (Invitrogen, Eugene, Oregon, USA), respectively

Flow cytometry and sorting of cytotoxic T lymphocytes

Stimulated PBMCs were incubated at 37°C for 15 min in the presence of Nef138-10(wt)/A24-APC or Nef138-10(2F)/A24-PE or both. The final concentrations of Nef138-10(wt)/A24-APC and Nef138-10(2F)-PE in monomer pMHC were 11 and 8 μg/ml, respectively.